

Neutrino physics

P. Hernández

IFIC, Universidad de València and CSIC, E-46071 Valencia, Spain

Abstract

The topics discussed in this lecture include: general properties of neutrinos in the SM, the theory of neutrino masses and mixings (Dirac and Majorana), neutrino oscillations both in vacuum and in matter, an overview of the experimental evidence for neutrino masses and of the prospects in neutrino oscillation physics. We also briefly review the relevance of neutrinos in leptogenesis and in beyond-the-Standard-Model physics.

1 Neutrinos in the Standard Model

LEP era established the validity of the Standard Model (SM) with an accuracy below the per cent level. The SM is based on the gauge group $SU(3) \times SU(2) \times U_Y(1)$ that is spontaneously broken to the subgroup $SU(3)_{color} \times U(1)_{em}$. All the fermions of the SM fall into irreducible representations of this group with the quantum numbers summarized in Table 1 [1].

Neutrinos are the most elusive particles of this table. They do not carry electromagnetic or colour charge, but only the weak charge under the spontaneously broken subgroup. For this reason they are extremely weakly interacting, since their interactions are mediated by massive gauge bosons.

The history of neutrinos goes back to W. Pauli who postulated the existence of the electron neutrino in an attempt to restore energy–momentum conservation in β decay, but he did so with great regret: *I have done a terrible thing, I have postulated a particle that cannot be detected*. Fortunately Pauli was wrong, not only have neutrinos been detected but they have been extremely useful in establishing the two most striking features of Table 1: the left–handedness of the weak interactions (the left–right asymmetry of the table) and the family structure (the three–fold repetition of the same representations).

In the SM only the left-handed fields carry the $SU(2)$ charge, where by left-handed we denote the negative chirality component (i.e., eigenstate of γ_5 with eigenvalue minus one) of the fermion field [1]:

$$\Psi = \underbrace{\Psi_R}_{P_R} + \underbrace{\Psi_L}_{P_L} = \left(\frac{1 + \gamma_5}{2} \right) \Psi + \left(\frac{1 - \gamma_5}{2} \right) \Psi. \quad (1)$$

For relativistic fermions (i.e., massless), it is easy to see that the chiral projectors are equivalent to the projectors on helicity components:

$$P_{R,L} = \frac{1}{2} \left(1 \pm \frac{\mathbf{s} \cdot \mathbf{p}}{|\mathbf{p}|} \right) + O\left(\frac{m_i}{E}\right), \quad (2)$$

where the helicity operator $\Sigma = \frac{\mathbf{s} \cdot \mathbf{p}}{|\mathbf{p}|}$ measures the component of the spin in the direction of the spatial momentum. Therefore for massless fermions only the left-handed states (with the spin pointing in the opposite direction to the momentum) carry $SU(2)$ charge. This is not inconsistent with Lorentz invariance, since for a fermion travelling at the speed of light, the helicity is the same in any reference frame. In other words, the helicity operator commutes with the Hamiltonian for a massless fermion and is thus a good quantum number.

The discrete symmetry under CPT (charge conjugation, parity, and time reversal), which is a basic building block of any Lorentz invariant and unitary field theory, requires that for any left-handed fermion, there exists a right-handed antiparticle, with opposite charge, but the right-handed particle state may not

Table 1: Irreducible fermionic representations in the Standard Model: $(I_{SU(3)}, I_{SU(2)})_Y$

$(\mathbf{1}, \mathbf{2})_{-\frac{1}{2}}$	$(\mathbf{3}, \mathbf{2})_{-\frac{1}{6}}$	$(\mathbf{1}, \mathbf{1})_{-1}$	$(\mathbf{3}, \mathbf{1})_{-\frac{2}{3}}$	$(\mathbf{3}, \mathbf{1})_{-\frac{1}{3}}$
$\begin{pmatrix} \nu_e \\ e \end{pmatrix}_L$	$\begin{pmatrix} u^i \\ d^i \end{pmatrix}_L$	e_R	u^i_R	d^i_R
$\begin{pmatrix} \nu_\mu \\ \mu \end{pmatrix}_L$	$\begin{pmatrix} c^i \\ s^i \end{pmatrix}_L$	μ_R	c^i_R	s^i_R
$\begin{pmatrix} \nu_\tau \\ \tau \end{pmatrix}_L$	$\begin{pmatrix} t^i \\ b^i \end{pmatrix}_L$	τ_R	t^i_R	b^i_R

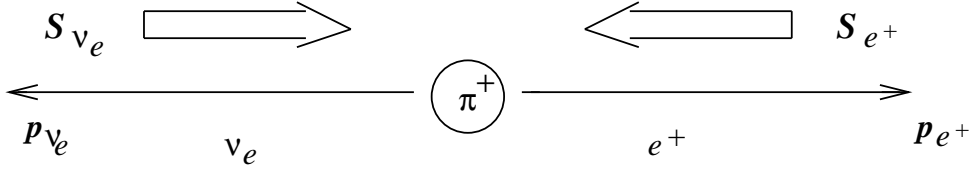


Fig. 1: Kinematics of pion decay

exist. This is precisely what happens with neutrinos in the SM. Since only the left-handed states carry charge and their masses were compatible with zero when the SM was established, they were postulated to be Weyl fermions: i.e., a left-handed particle and a right-handed antiparticle.

Under parity, a left-handed particle state transforms into a right-handed particle state, thus the left-handedness of the weak interactions implies a maximal violation of parity, which is nowhere more obvious than in the neutrino sector, where the reflection of a SM neutrino in a mirror is nothing.

The weak current is therefore $V - A$ since it only couples to the left fields: $\bar{\Psi}_L \gamma_\mu \Psi_L = \bar{\Psi} \gamma_\mu (1 - \gamma_5)/2 \Psi$. This structure is clearly seen in the kinematics of weak decays involving neutrinos, such as the classic example of pion decay to $e\nu_e$ or $\mu\nu_\mu$. In the limit of vanishing electron or muon mass, this decay is forbidden, because the spin of the initial state is zero and thus it is impossible to conserve simultaneously momentum and angular momentum if the two recoiling particles must have opposite helicities, as shown in Fig. 1. Thus the ratio of the decay rates to electrons and muons, in spite of the larger phase space in the former, is strongly suppressed by the factor $\left(\frac{m_e}{m_\mu}\right)^2 \sim 2 \times 10^{-5}$.

Another profound consequence of the chiral nature of the weak interaction is anomaly cancellation. The chiral coupling of fermions to gauge fields leads generically to inconsistent gauge theories due to chiral anomalies: if any of the diagrams depicted in Fig. 2 is non-vanishing, the weak current is conserved at tree level but not at one loop, implying a catastrophic breaking of gauge invariance. Anomaly cancellation is the requirement that all these diagrams vanish, which imposes strong constraints on the hypercharge assignments of the fermions in the SM, which are *miraculously* satisfied:

$$\overbrace{\sum_{i=\text{quarks}} Y_i^L - Y_i^R}^{GGB} = \overbrace{\sum_{i=\text{doublets}} Y_i^L}^{WWB} = \overbrace{\sum_i Y_i^L - Y_i^R}^{Bgg} = \overbrace{\sum_i (Y_i^L)^3 - (Y_i^R)^3}^{B^3} = 0, \quad (3)$$

where $Y_i^{L/R}$ are the hypercharges of the left/right components of the fermionic field i , and the triangle diagram corresponding to each of the sums is indicated above the bracket.

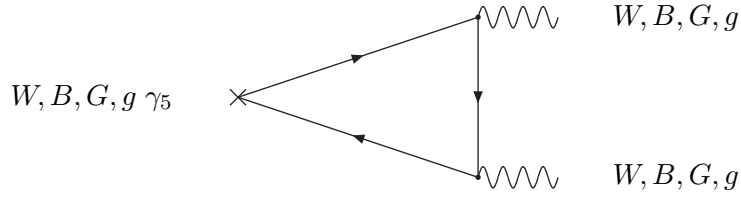


Fig. 2: Triangle diagrams that can give rise to anomalies. W, B, G are the gauge bosons associated to the $SU(2), U_Y(1), SU(3)$ gauge groups, respectively, and g is the graviton

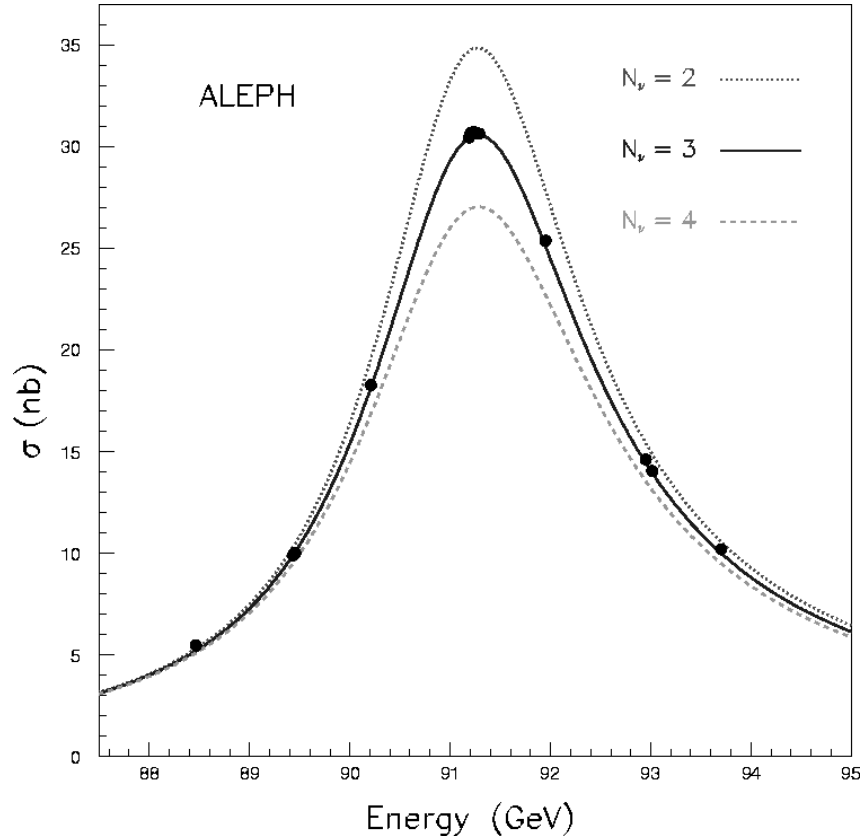


Fig. 3: Z^0 resonance from the ALEPH experiment at LEP. Data are compared to the case of $N_\nu = 2, 3$ and 4

Concerning the family structure, we know, thanks to neutrinos, that there are exactly three families in the SM. An extra SM family with quarks and charged leptons so heavy that they remain unobserved, would also have massless neutrinos that would have been produced in Z^0 decay, modifying its width, which has been measured at LEP with an impressive precision, as shown in Fig. 3. This measurement excludes any number of standard neutrino families different from three [2]:

$$N_\nu = 2.984 \pm 0.008. \quad (4)$$

2 Neutrino masses and mixings

When the SM was invented, there were only upper limits on the neutrino masses so these were conjectured to be zero. The direct limit on neutrino masses comes from the precise measurement of the end-point of the lepton energy spectrum in weak decays, which gets modified if neutrinos are massive.

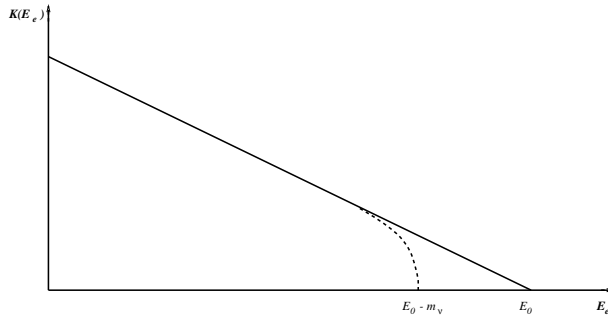


Fig. 4: Effect of a neutrino mass in the end-point of the lepton energy spectrum in β decay

In particular the most stringent limit is obtained from tritium β -decay for the electron neutrino:

$$H^3 \rightarrow {}^3He + e^- + \bar{\nu}_e. \quad (5)$$

Figure 4 shows the effect of a neutrino mass in the end-point electron energy spectrum in this decay. The functional form of this curve is $K(E_e) \propto \sqrt{(E_0 - E_e)((E_0 - E_e)^2 - m_\nu^2)^{1/2}}$. The best limit has been obtained by the Mainz and Troitsk experiments [3]:

$$m_{\nu_e} < 2.2 \text{ eV (Mainz)}, \quad m_{\nu_e} < 2.1 \text{ eV (Troitsk)}, \quad (6)$$

both at 95% CL. The direct limits on the other two neutrino masses are much weaker. The best limit on the ν_μ mass ($m_{\nu_\mu} < 170 \text{ keV}$ [4]) was obtained from the end-point spectrum of the decay $\pi^+ \rightarrow \mu^+ \nu_\mu$, while that on the ν_τ mass was obtained at LEP ($m_{\nu_\tau} < 18.2 \text{ MeV}$ [5]) from the decay $\tau \rightarrow 5\pi \nu_\tau$.

As we shall see, there is now strong evidence that neutrinos are indeed massive, although extremely light, below the stringent bound of Eq. (6).

Neutrino masses can be easily accommodated in the SM. A massive fermion necessarily has two states of helicity, since it is always possible to reverse the helicity of a state that moves at a slower speed than light by looking at it from a boosted reference frame. In fact a mass can be thought of as the strength of the coupling between the two helicity states:

$$m \overline{\psi}_L \psi_R + \text{h.c.} \quad (7)$$

In order to include such a coupling in the SM for the neutrinos we need to identify the neutrino right-handed state, which in the SM is absent. It turns out there are two ways to proceed:

Dirac massive neutrinos

We can enlarge the SM by adding a set of three right-handed neutrino states, which would be singlets under $SU(3) \times SU(2) \times U_Y(1)$, but coupled to matter just through the neutrino masses. This coupling has to be of the Yukawa type to preserve the gauge symmetry in such a way that the masses are proportional to the vacuum expectation value of the Higgs field, v , exactly like for the remaining fermions [1]:

$$\lambda_\nu \overline{L}_L \tilde{\Phi} \nu_R + \text{h.c.} \rightarrow m_\nu = \lambda_\nu v, \quad (8)$$

where $L_L = (\nu_L \ l_L)$ is the lepton doublet and $\tilde{\Phi}$ is the scalar doublet that gets a vacuum expectation value $\langle \tilde{\Phi} \rangle = (v \ 0)$. There are two important consequences of proceeding in this way. Firstly there is a new hierarchy problem in the SM to be explained: why neutrinos are much lighter than the remaining leptons, even those in the same family (see Fig. 5). Secondly, lepton number, L , which counts the number of leptons minus that of antileptons, remains an exactly conserved global symmetry at the classical level¹, just as baryon number, B , is.

¹As usual $B + L$ is broken by the anomaly and only $B - L$ remains exact at all orders.

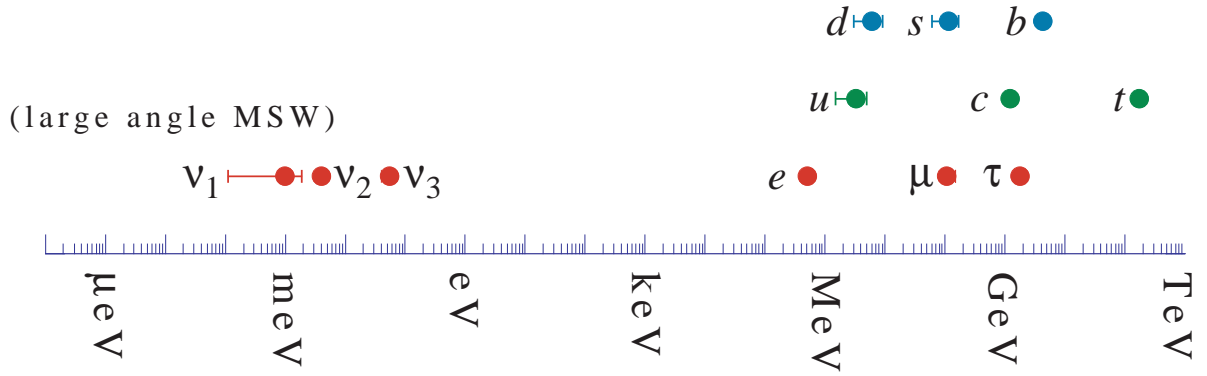


Fig. 5: Fermion spectrum in the Standard Model

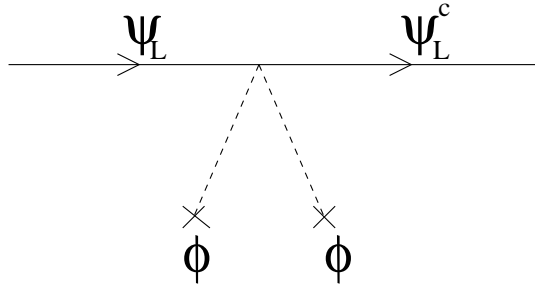


Fig. 6: Majorana coupling of the light neutrinos to the Higgs field

Majorana massive neutrinos

For neutral particles, Majorana realized that one can get rid of half of the degrees of freedom in a massive Dirac spinor in a Lorentz-invariant way by identifying the right-handed state with the antiparticle of the left-handed state:

$$\nu_R \rightarrow (\nu_L)^c = C\bar{\nu}_L^T = C\gamma_0\nu_L^*, \tag{9}$$

where C is the operator of charge conjugation in spinor space.

Neutrinos are the only particles for which this possibility is compatible with charge conservation, because they are charged only under the spontaneously broken subgroup of the SM and thus a Majorana mass term can be written in a gauge invariant way by including two Higgs fields, as shown in Fig. 6:

$$\frac{1}{M}L_L^T C \alpha_\nu \tilde{\Phi}^T \tilde{\Phi} L_L + \text{h.c.}, \tag{10}$$

where an energy scale, M , has been introduced for dimensional reasons, so that the coupling α_ν is adimensional. Upon spontaneous symmetry breaking, these couplings become Majorana neutrino masses of the form

$$m_\nu = \alpha_\nu \frac{v^2}{M}. \tag{11}$$

If the scale M is much higher than the electroweak scale v , a strong hierarchy between the neutrino and the charged lepton masses arises naturally.

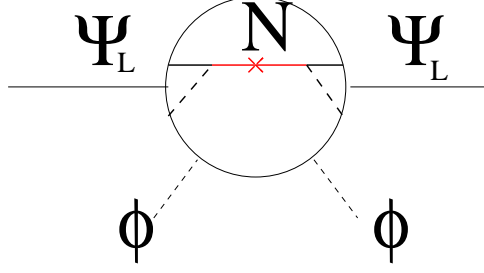


Fig. 7: Neutrino masses in the see-saw model

2.1 See-saw models

It is interesting to consider the simplest example to explain the origin of the scale M in the Majorana masses. This is the famous see-saw model of Gell-Mann, Ramond, Slansky, and Yanagida [6]. In this model, the Majorana effective interaction of Eq. (10) results from the interchange of very heavy right-handed Majorana neutrinos, as depicted in Fig. 7. The SM Lagrangian is enlarged with the terms

$$\delta\mathcal{L}_Y^\nu = \bar{L}_L \tilde{\lambda}_\nu \tilde{\Phi} N_R + \frac{1}{2} N_R^T C M_R N_R + \text{h.c.}, \quad (12)$$

that is a Yukawa coupling of the lepton doublet and the heavy singlets plus a Majorana mass term for the singlets. Upon spontaneous symmetry breaking these couplings become mass terms:

$$\delta\mathcal{L}_Y^\nu \rightarrow \frac{1}{2} (\nu_L^T \quad N_R^T) C \begin{pmatrix} 0 & \tilde{\lambda}_\nu v \\ \tilde{\lambda}_\nu^T v & M_R \end{pmatrix} \begin{pmatrix} \nu_L \\ N_R \end{pmatrix}. \quad (13)$$

When $v \ll M_R$, the diagonalization of the mass matrix can be done in perturbation theory:

$$\mathcal{M} = \mathcal{M}^{(0)} + \mathcal{M}^{(1)} \equiv \begin{pmatrix} 0 & 0 \\ 0 & M_R \end{pmatrix} + \begin{pmatrix} 0 & \tilde{\lambda}_\nu v \\ \tilde{\lambda}_\nu^T v & 0 \end{pmatrix}. \quad (14)$$

To second order we find:

$$U^T \mathcal{M} U = \begin{pmatrix} -v^2 \tilde{\lambda}_\nu \frac{1}{M_R} \tilde{\lambda}_\nu^T & 0 \\ 0 & M_R \end{pmatrix} \quad U = \begin{pmatrix} 1 & \tilde{\lambda}_\nu \frac{v}{M_R} \\ -\frac{v}{M_R} \tilde{\lambda}_\nu^T & 1 \end{pmatrix}. \quad (15)$$

There are three light Majorana neutrinos ($\nu'_L \simeq \nu_L + \tilde{\lambda}_\nu \frac{v}{M_R} N_R$) with a mass matrix:

$$v^2 \tilde{\lambda}_\nu \frac{1}{M_R} \tilde{\lambda}_\nu^T, \quad (16)$$

and three heavy ones ($N'_R \simeq N_R - \frac{v}{M_R} \tilde{\lambda}_\nu^T \nu_L$) with the mass matrix M_R .

Equivalently we say that the heavy Majoranas can be integrated out leaving a trace of higher dimensional operators:

$$\mathcal{L}_{eff}^{d=5} = \frac{1}{2} L_L^T C \tilde{\Phi}^T \left(\tilde{\lambda}_\nu \frac{1}{M_R} \tilde{\lambda}_\nu^T \right) \tilde{\Phi} L_L \quad (17)$$

$$\mathcal{L}_{eff}^{d=6} = \mathcal{O} \left(\frac{1}{M_R^2} \right) \dots \quad (18)$$

The one with lowest dimension is the one we obtained from symmetry arguments in Eq. (10).

A few observations are in place:

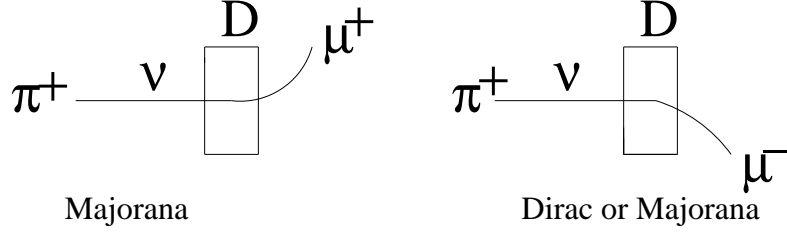


Fig. 8: A neutrino beam from π^+ decay (ν_μ) could interact in the magnetized detector producing a μ^+ only if neutrinos are Majorana.

- The new physics scale M in Eq. (10) is simply related to the masses of the heavy Majorana neutrinos and the Yukawa couplings:

$$\frac{\alpha_\nu}{M} \rightarrow \tilde{\lambda}_\nu \frac{1}{M_R} \tilde{\lambda}_\nu^T. \quad (19)$$

As we shall see, data imply there is at least one $m_\nu \geq 0.05$ eV. If $\tilde{\lambda}_\nu \sim O(1)$ then:

$$v < M_R \sim 10^{15} \text{ GeV} < M_{\text{Planck}}, \quad (20)$$

and the masses are close to the typical Grand Unification (GUT) scale.

- In order to give non-vanishing masses to all the three left-handed neutrinos, the number of Majorana singlets must satisfy $N_R \geq N_L = 3$. The reason is that the matrix $\underbrace{\tilde{\lambda}_\nu}_{N_L \times N_R} \underbrace{\frac{1}{M_R}}_{N_R \times N_R} \underbrace{\tilde{\lambda}_\nu^T}_{N_R \times N_L}$ has $N_L - N_R$ zero modes.

2.2 Majorana versus Dirac

The consequences of the SM neutrinos being massive Majorana particles are profound:

- A new physics scale M must exist and is accessible in an indirect way through neutrino masses.
- Lepton number is not conserved: a Majorana mass violates the conservation of all the charges carried by the fermion, including the global charges such as lepton number. As we shall see in Section 6, the dynamics associated to the scale M could be responsible for the generation of the baryon asymmetry in the Universe.
- The anomaly cancellation conditions fix all the hypercharges (i.e., there is only one possible choice for the hypercharges that satisfies Eq. (3)), which implies that electromagnetic charge quantization is the only possibility in a field theory with the same matter content as the SM.

It is clear that establishing the Majorana nature of neutrinos is of great importance. In principle there are very clear signatures, such as the one depicted in Fig. 8, where a ν_μ beam from π^+ decay is intercepted by a detector. In the Dirac case, the interaction of neutrinos on the detector via a charged current interaction will produce a μ^- in the final state. If neutrinos are Majorana, a wrong-sign muon in the final state is also possible. Unfortunately the rate for μ^+ production is suppressed by m_ν/E in amplitude with respect to the μ^- . For example, for $E_\nu = O(1)$ GeV and $m_\nu \sim O(1)$ eV the cross-section for this process will be roughly 10^{-18} times the usual CC neutrino cross-section, which means it is impossible to detect.

The best hope of observing a rare process of this type seems to be the search for neutrinoless double-beta decay ($2\beta 0\nu$), the right diagram of Fig. 9. The background to this process is the standard

Experiment	Nucleus	$ m_{ee} $
Heidelberg-Moscow I	^{76}Ge	$< 0.34\text{--}1.1 \text{ eV}(90\% \text{ CL})$ [9]
Heidelberg-Moscow II	^{76}Ge	$0.2\text{--}0.6 \text{ eV}$ [10]
CUORICINO	^{120}Te	$< 0.2\text{--}1.1 \text{ eV}(90\% \text{ CL})$ [11]
NEMO-3	^{100}Mo	$< 0.6\text{--}2 \text{ eV}(90\% \text{ CL})$ [12]

Table 2: Present bounds from various neutrinoless double-beta-decay experiments

double-beta decay depicted on the left of Fig. 9, which has been observed to take place with a lifetime of $T_{2\beta 2\nu} > 10^{19}\text{--}10^{21}$ years.

If the source of L violation is just the Majorana ν mass, the inverse lifetime for this process is given by

$$T_{2\beta 0\nu}^{-1} \simeq \underbrace{G^{0\nu}}_{\text{Phase}} \underbrace{|M^{0\nu}|^2}_{\text{Nuclear M.E.}} \underbrace{\left| \sum_i (V_{MNS}^{ei})^2 m_i \right|^2}_{|m_{ee}|^2}, \quad (21)$$

where m_{ee} is the 11 entry in the neutrino mass matrix in the flavour basis. In spite of the suppression in the neutrino mass (over the energy of this process), the neutrinoless mode has a larger phase factor than the 2ν mode, and as a result the lifetime is expected to be of the order

$$T_{2\beta 0\nu}^{-1} \sim \left(\frac{m_\nu}{E}\right)^2 10^9 T_{2\beta 2\nu}^{-1}, \quad (22)$$

which could be observable for neutrino masses in the eV range. Several experiments have set stringent upper bounds on $|m_{ee}|$ and there is even a controversial positive signal, as shown in Table 2.

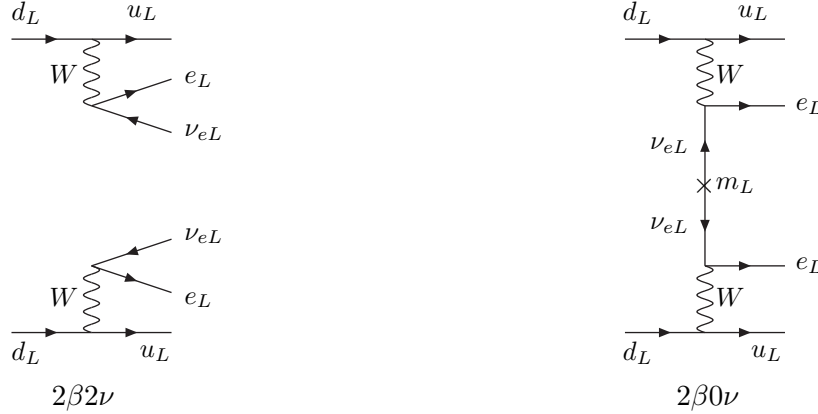


Fig. 9: 2β decay: normal (left) and neutrinoless (right)

2.3 Neutrino mixing

Generically, neutrino masses imply neutrino mixing [7, 8], because the Yukawa couplings need not be flavour diagonal:

$$\mathcal{L}_m^{\text{Dirac}} = \overline{\nu}_L^i (\lambda_\nu v)_{ij} \nu_R^j + \text{h.c.} \quad (23)$$

$$\mathcal{L}_m^{\text{Majorana}} = \frac{1}{2} \frac{v^2}{M} \nu_L^i T C (\alpha_\nu)_{ij} \nu_L^j + \text{h.c.} \quad (24)$$

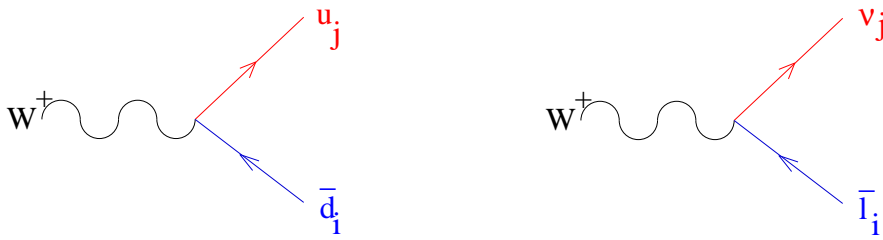


Fig. 10: Quark and lepton mixing

Instead, in the mass eigenbasis for all the leptons, the charged weak couplings are not diagonal, in complete analogy with the quark flavour sector (see Fig. 10):

$$\mathcal{L}^{\text{Dirac}} = \bar{l}_L^i \gamma_\mu W_\mu^+ V_{\text{MNS}}^{ij} \nu_L^j + \frac{1}{2} \bar{\nu}_L^i \gamma_\mu Z_\mu \nu_L^i + \bar{\nu}_L^i m_i \nu_R^i + \text{h.c.} \quad (25)$$

$$\mathcal{L}^{\text{Majorana}} = \bar{l}_L^i \gamma_\mu W_\mu^+ \tilde{V}_{\text{MNS}}^{ij} \nu_L^j + \frac{1}{2} \bar{\nu}_L^i \gamma_\mu Z_\mu \nu_L^i + \frac{1}{2} \nu_L^i{}^T C m_i \nu_L^i + \text{h.c.} \quad (26)$$

The number of parameters that are in principle observable in the lepton mixing matrix (V_{MNS} for Dirac and \tilde{V}_{MNS} for Majorana) can easily be computed by counting the number of independent real and imaginary elements of the Yukawa matrices and eliminating those that can be absorbed in field redefinitions. The allowed field redefinitions are the unitary rotations of the fields that leave the Lagrangian invariant in the absence of lepton masses, but are not symmetries of the full Lagrangian when lepton masses are included.

In the Dirac case, it is possible to rotate independently the left-handed lepton doublet, together with the right-handed charged leptons and neutrinos, that is $U(n)^3$, for a generic number of families n . However, this includes total lepton number which remains a symmetry of the massive theory and thus cannot be used to reduce the number of physical parameters in the mass matrix. The parameters that can be absorbed in field redefinitions are thus the parameters of the group $U(n)^3/U(1)$ (that is $\frac{3(n^2-n)}{2}$ real, $\frac{3(n^2+n)-1}{2}$ imaginary).

In the case of Majorana neutrinos, there is no independent right-handed neutrino field, nor is lepton number a good symmetry. Therefore the number of field redefinitions is the number of parameters of the elements in $U(n)^2$ (that is $n^2 - n$ real and $n^2 + n$ imaginary).

The resulting real physical parameters are the mass eigenstates and the mixing angles, while the resulting imaginary parameters are CP-violating phases. All this is summarized in Table 3. Dirac and Majorana neutrinos differ only in the number of observable phases. For three families ($n = 3$), there is just one Dirac phase and three in the Majorana case.

A standard parametrization of the mixing matrices is given by

$$V_{\text{MNS}} = \begin{pmatrix} 1 & 0 & 0 \\ 0 & c_{23} & s_{23} \\ 0 & -s_{23} & c_{23} \end{pmatrix} \begin{pmatrix} c_{13} & 0 & s_{13} \\ 0 & 1 & 0 \\ -s_{13} & 0 & c_{13} \end{pmatrix} \begin{pmatrix} c_{12} & s_{12}e^{i\delta} & 0 \\ -s_{12}e^{i\delta} & c_{12} & 0 \\ 0 & 0 & 1 \end{pmatrix} \quad (27)$$

$$\tilde{V}_{\text{MNS}} = V_{\text{MNS}}(\theta_{12}, \theta_{13}, \theta_{23}, \delta) \begin{pmatrix} 1 & 0 & 0 \\ 0 & e^{i\alpha_1} & 0 \\ 0 & 0 & e^{i\alpha_2} \end{pmatrix}. \quad (28)$$

3 Neutrino oscillations

The fact that neutrinos are such weakly interacting particles allows them to have coherence over very long distances. For example, a neutrino with an energy of $\mathcal{O}(1 \text{ MeV})$ moving in lead, which has a

Table 3: Number of real and imaginary parameters in the Yukawa matrices, of those that can be absorbed in field redefinitions. The difference between the two is the number of observable parameters: the lepton masses (m), mixing angles (θ), and phases (ϕ).

	Yukawas	Field redefinitions	No. m	No. θ	No. ϕ
Dirac	λ_l, λ_ν $4n^2$	$U(n)^3/U(1)_L$ $\frac{3(n^2 - n)}{2}, \frac{3(n^2 + n) - 1}{2}$	$2n$	$\frac{n^2 - n}{2}$	$\frac{(n - 2)(n - 1)}{2}$
Majorana	$\lambda_l, \alpha_\nu^T = \alpha_\nu$ $3n^2 + n$	$U(n)^2$ $n^2 - n, n^2 + n$	$2n$	$\frac{n^2 - n}{2}$	$\frac{n^2 - n}{2}$

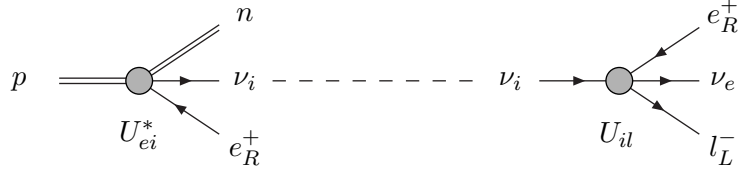


Fig. 11: Neutrino oscillations

density of $\rho = 7.9 \text{ g/cm}^3$, has a mean free path $l \sim \frac{1}{\sigma\rho} \sim 4 \times 10^{16}$ metres ~ 4 light-years.

Neutrinos are necessarily produced in a flavour eigenstate, that is, in a precise combination of the mass eigenstates, which are the true eigenstates of the free Hamiltonian. After some distance L , where neutrinos have evolved freely, the mass eigenstate components in the original flavour state get different phases and, as a result, there is a non-zero probability that the flavour measured at L is a different one [7], as shown in Fig. 11.

There has been a lot of discussion about what is the rigorous way to define such a transition probability. This is not straightforward because, in quantum field theory (which is required since neutrinos are relativistic), we are used to considering processes in which there is no knowledge of the position in space or time where the interaction took place, and it is then a good approximation to consider asymptotic states that are simply plane waves, with well-defined energy–momentum. In this case this is not possible, because we must distinguish the macroscopic distance that separates the source of neutrinos and the detector. This implies that it cannot be a good approximation to consider asymptotic states of well-defined momentum at least in the direction between source and detector. This fact has often confused the derivation and even led to incorrect results.

Let us consider that neutrinos are produced as wave packets localized around the source position $x_0 = (t_0, \mathbf{x}_0)$ in a flavour state α :

$$|\nu_\alpha(x)\rangle = \sum_j V_{\alpha j} \int \frac{d^3k}{(2\pi)^3} f_j(\mathbf{k}) e^{-ik_0^j(t-t_0)} e^{i\mathbf{k}(\mathbf{x}-\mathbf{x}_0)} |\nu_j\rangle, \quad (29)$$

where $k_0^{j2} = \mathbf{k}^2 + m_j^2$, since the state being asymptotic must be on-shell and $V_{\alpha j}$ is the mixing matrix. The wave packets $f_j(\mathbf{k})$ depend on the production process (uncertainty in momentum of the initial states, kinematics), but we do not need to know the exact form. For example we can consider a Gaussian:

$$f_i(\mathbf{k}) \sim e^{-(\mathbf{k}-\bar{\mathbf{q}}^i)^2/(2\sigma_i^2)}. \quad (30)$$

We expect that, neglecting neutrino masses, the wave packets are the same for all the mass eigenstates:

$$f_i(\mathbf{k}) \sim f(\mathbf{k}) + O(m_i/|\mathbf{k}|) \sim e^{-(\mathbf{k}-\mathbf{q})^2/(2\sigma^2)}. \quad (31)$$

Let us forget about the proper normalization of the state for the time being. Let us consider that the neutrino produced is moving in the direction of a detector located at some distance down the beam line L in the \hat{z} direction (therefore $\mathbf{q} = (0, 0, q_z)$), where we want to measure the flavour of the state in Eq. (29). The probability that we measure a state with flavour β at any point x is $\sim |\langle \nu_\beta | \nu_\alpha(x) \rangle|^2$, where

$$|\nu_\beta\rangle = \sum_j V_{\beta j} |\nu_j\rangle. \quad (32)$$

The amplitude is then

$$\langle \nu_\beta | \nu_\alpha(x) \rangle = \sum_i V_{\beta i}^* V_{\alpha i} \int d^3k f_i(\mathbf{k}) e^{-ik_0^i(t-t_0)} e^{i\mathbf{k}(\mathbf{x}-\mathbf{x}_0)}. \quad (33)$$

Note that we measure neither the time of the measurement nor the spatial \hat{x} and \hat{y} components, so we can integrate over them:

$$P(\nu_\alpha \rightarrow \nu_\beta) \sim \int dt d\hat{x} d\hat{y} |\langle \nu_\beta | \nu_\alpha(x) \rangle|^2 = \sum_{i,j} V_{\beta i}^* V_{\alpha i} V_{\beta j} V_{\alpha j}^* \times \int_{\mathbf{k}} \int_{\mathbf{k}'} dk'_z f_i(\mathbf{k}) f_j^*(\mathbf{k}') \delta\left(\sqrt{m_i^2 + k_z^2 + k_x^2 + k_y^2} - \sqrt{m_j^2 + k_z'^2 + k_x^2 + k_y^2}\right) e^{i(k_z - k_z')L}. \quad (34)$$

Up to exponentially small terms and neglecting effects of $O(m_i/|\mathbf{k}|)$ everywhere else than in the phase factor (where they are enhanced by L), we obtain

$$P(\nu_\alpha \rightarrow \nu_\beta) \sim \sum_{i,j} V_{\beta i}^* V_{\alpha i} V_{\beta j} V_{\alpha j}^* \int_{\mathbf{k}} |f(\mathbf{k})|^2 \frac{|\mathbf{k}|}{|k_z|} e^{-i \frac{\Delta m_{ji}^2 L}{2|k_z|}}, \quad (35)$$

where $\Delta m_{ji}^2 = m_i^2 - m_j^2$.

Now, we have to care about the normalization. The simplest way to compute it is by requiring that the probability be one if $\alpha = \beta$ in the case of zero or equal neutrino masses (i.e., $\Delta m_{ji}^2 = 0$). Doing this we finally obtain

$$P(\nu_\alpha \rightarrow \nu_\beta) = \sum_{i,j} V_{\beta j}^* V_{\alpha j} V_{\beta i} V_{\alpha i}^* \int_{\mathbf{k}} e^{-i \frac{\Delta m_{ij}^2 L}{2|k_z|}} \frac{|\mathbf{k}|}{|k_z|} |f(\mathbf{k})|^2 / \int_{\mathbf{k}} \frac{|\mathbf{k}|}{|k_z|} |f(\mathbf{k})|^2 \simeq \sum_{i,j} V_{\beta j}^* V_{\alpha j} V_{\beta i} V_{\alpha i}^* e^{-i \frac{\Delta m_{ij}^2 L}{2|q_z|}}, \quad (36)$$

where in the last equality we have assumed that the phase factor does not change very much in the range of momenta of the wave packet, so that it can be taken out of the integral. The probability for the flavour transition is thus a periodic function of the distance between source and detector, hence the name *neutrino oscillations* first described by Pontecorvo [7].

Defining $W_{\alpha\beta}^{jk} \equiv [V_{\alpha j} V_{\beta j}^* V_{\alpha k}^* V_{\beta k}]$ and using the unitarity of the mixing matrix, we can rewrite the probability in the more familiar way:

$$P(\nu_\alpha \rightarrow \nu_\beta) = \delta_{\alpha\beta} - 4 \sum_{k>j} \text{Re}[W_{\alpha\beta}^{jk}] \sin^2\left(\frac{\Delta m_{jk}^2 L}{4E_\nu}\right) \quad (37)$$

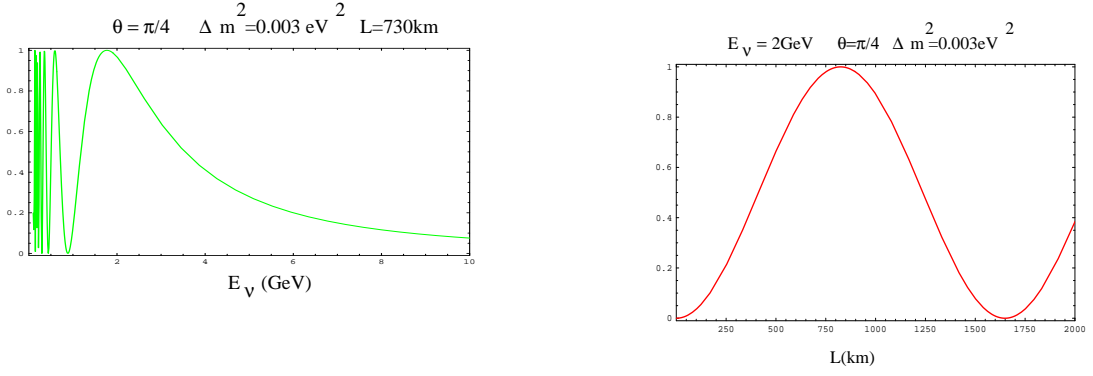


Fig. 12: Two-family oscillation probability as a function of the neutrino energy at fixed baseline of $L = 730$ km (left) and as a function of the baseline at fixed neutrino energy $E_\nu = 2$ GeV (right)

$$\pm 2 \sum_{k>j} \text{Im}[W_{\alpha\beta}^{jk}] \sin\left(\frac{\Delta m_{jk}^2 L}{2E_\nu}\right), \quad (38)$$

where the \pm refers to neutrinos/antineutrinos and $|\mathbf{q}| = |q_z| \simeq E_\nu$.

We refer to an *appearance* or *disappearance* oscillation probability when the initial and final flavours are different ($\alpha \neq \beta$) or the same ($\alpha = \beta$), respectively. Note that oscillation probabilities show the expected GIM suppression of any flavour changing process: they vanish if the neutrinos are degenerate.

In the simplest case of two-family mixing, the mixing matrix depends on just one mixing angle:

$$V_{\text{MNS}} = \begin{pmatrix} \cos \theta & \sin \theta \\ -\sin \theta & \cos \theta \end{pmatrix}, \quad (39)$$

and there is only one mass square difference Δm^2 . The oscillation probability of Eq. (38) simplifies to the well-known expression

$$P(\nu_\alpha \rightarrow \nu_\beta) = \sin^2 2\theta \sin^2\left(\frac{\Delta m^2 L}{4E_\nu}\right), \quad \alpha \neq \beta. \quad (40)$$

The probability is the same for neutrinos and antineutrinos because there are no imaginary entries in the mixing matrix. It is a sinusoidal function of the distance between source and detector, with a period determined by the oscillation length:

$$L_{\text{osc}} (\text{km}) = 2\pi \frac{E_\nu (\text{GeV})}{1.27 \Delta m^2 (\text{eV}^2)}, \quad (41)$$

which is proportional to the neutrino energy and inversely proportional to the neutrino mass square difference. The amplitude of the oscillation is determined by the mixing angle. It is maximal for $\sin^2 2\theta = 1$ or $\theta = \pi/4$. This oscillation probability as a function of the neutrino energy and the baseline is shown in Fig. 12

It is important to stress that there is an intrinsic limit to coherence, since the size of the wave packet is non-zero. Indeed the last equality of Eq. (36) requires that the phase factor varies slowly in the range of momenta of the wave packet. This condition is not satisfied when L becomes too large. The decoherence length, L_D , can be estimated as

$$\left| \frac{\Delta m_{ij}^2 L_D}{2} \left(\frac{1}{|q_z|} - \frac{1}{|q_z| + \sigma} \right) \right| \sim 2\pi \Rightarrow L_D \sim L_{\text{osc}} \frac{|q_z|}{\sigma}. \quad (42)$$

that is the phase factor changes by 2π when the momentum in the \hat{z} direction varies within one σ from the central value, where σ is the width of the wave packet in momentum space [see Eq. (30)] When the baseline satisfies $L \gg L_D$, neutrinos do not oscillate because the phase factor averages to zero all the terms with $i \neq j$ in Eq. (36). The flavour transition probability then becomes independent of L :

$$P(\nu_\alpha \rightarrow \nu_\beta) = \sum_i |V_{\alpha i} V_{\beta i}|^2 = 2 \cos^2 \theta \sin^2 \theta = \frac{1}{2} \sin^2 2\theta. \quad (43)$$

In practice, the smearing in L and E_ν produces the same effect. When $L \gg L_{\text{osc}}$, the oscillations are so fast that any real experiment will measure the average:

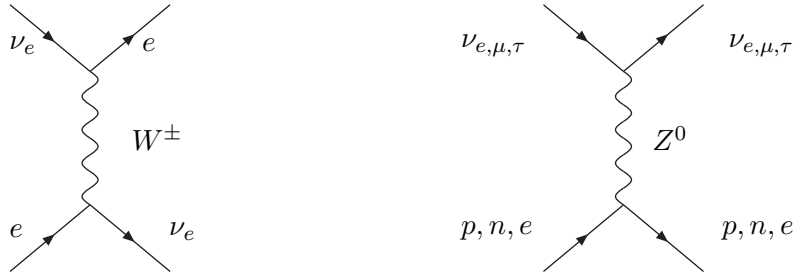
$$\langle P(\nu_\alpha \rightarrow \nu_\beta) \rangle = \frac{1}{2} \sin^2 2\theta, \quad (44)$$

which is exactly the same result as in the case of no coherence.

Note that the 'smoking gun' for neutrino oscillations is not the flavour transition, which can occur in the presence of neutrino mixing without oscillations, but the peculiar L/E_ν dependence. An idealized experiment looking for neutrino oscillations should then be able to tell flavour on one hand and should be performed at a baseline such that $L \sim L_{\text{osc}}(E_\nu)$ in order to observe the oscillatory pattern, which measures the neutrino mass square difference. Note that neutrino oscillations are not sensitive to the absolute mass scale though.

3.1 Matter effects

When neutrinos propagate in matter (Earth, Sun, etc.), the amplitude for their propagation is modified owing to coherent forward scattering on electrons and nucleons [13]:



The effective Hamiltonian density resulting from the charged current interaction is

$$\mathcal{H}_{\text{CC}} = \sqrt{2}G_F [\bar{e}\gamma_\mu P_L \nu_e][\bar{\nu}_e \gamma^\mu P_L e] = \sqrt{2}G_F [\bar{e}\gamma_\mu P_L e][\bar{\nu}_e \gamma^\mu P_L \nu_e]. \quad (45)$$

Since the medium is not polarized, the expectation value of the electron current is simply the number density of electrons:

$$\langle \bar{e}\gamma_\mu P_L e \rangle_{\text{unpol. medium}} = \delta_{\mu 0} N_e. \quad (46)$$

Including also the neutral current interactions in the same way, the effective Hamiltonian for neutrinos in the presence of matter is

$$\mathcal{H}^{\text{eff}} = \mathcal{H}^{\text{vac}} + \bar{\nu} V_m \gamma^0 (1 - \gamma_5) \nu \quad (47)$$

$$V_m = \begin{pmatrix} \left(\frac{G_F}{\sqrt{2}}\right) \left(N_e - \frac{N_n}{2}\right) & 0 & 0 \\ 0 & \frac{G_F}{\sqrt{2}} \left(-\frac{N_n}{2}\right) & 0 \\ 0 & 0 & \frac{G_F}{\sqrt{2}} \left(-\frac{N_n}{2}\right) \end{pmatrix}, \quad (48)$$

where N_n is the number density of neutrons. The matter potential in the center of the Sun is $V_e \sim 10^{-11}$ eV and in the Earth $V_e \sim 10^{-13}$ eV. In spite of these tiny values, these effects are non-negligible in neutrino oscillations.

The plane wave solutions to the modified Dirac equation satisfy a different dispersion relation and as a result, the phases of neutrino oscillation phenomena change. The new dispersion relation becomes

$$E - V_m - M_\nu = (\pm|\mathbf{p}| - V_m) \frac{1}{E + M_\nu - V_m} (\pm|\mathbf{p}| - V_m) \quad h = \pm, \quad (49)$$

where $h = \pm$ indicate the two helicity states and we have neglected effects of $\mathcal{O}(VM_\nu)$. This is a reasonable approximation since $m_\nu \gg V_m$. For the positive energy states we then have

$$E > 0 \quad E^2 = |\mathbf{p}|^2 + M_\nu^2 + 4EV_m \quad h = - \quad E^2 = |\mathbf{p}|^2 + M_\nu^2, \quad h = +, \quad (50)$$

while for the negative energy ones $V_m \rightarrow -V_m$ and $h \rightarrow -h$.

The effect of matter can be simply accommodated in an effective mass matrix:

$$\tilde{M}_\nu^2 = M_\nu^2 \pm 4EV_m. \quad (51)$$

The effective mixing matrix \tilde{V}_{MNS} is the one that takes us from the original flavour basis to that which diagonalizes this effective mass matrix:

$$\begin{pmatrix} \tilde{m}_1^2 & 0 & 0 \\ 0 & \tilde{m}_2^2 & 0 \\ 0 & 0 & \tilde{m}_3^2 \end{pmatrix} = \tilde{V}_{\text{MNS}}^\dagger \left(M_\nu^2 \pm 4E \begin{pmatrix} V_e & 0 & 0 \\ 0 & V_\mu & 0 \\ 0 & 0 & V_\tau \end{pmatrix} \right) \tilde{V}_{\text{MNS}}. \quad (52)$$

Note that the number of physical parameters is the same but the effective mixing angles and masses depend on the energy.

3.2 Neutrino oscillations in constant matter

In the case of two flavours, the effective mass and mixing angle have relatively simple expressions:

$$\sin^2 2\tilde{\theta} = \frac{(\Delta m^2 \sin 2\theta)^2}{(\Delta m^2 \cos 2\theta \mp 2\sqrt{2} G_F E N_e)^2 + (\Delta m^2 \sin 2\theta)^2} \quad (53)$$

$$\Delta \tilde{m}^2 = \sqrt{(\Delta m^2 \cos 2\theta \mp 2\sqrt{2} E G_F N_e)^2 + (\Delta m^2 \sin 2\theta)^2}, \quad (54)$$

where the sign \mp corresponds to neutrinos/antineutrinos. The corresponding oscillation amplitude has a resonance [13, 14], when the neutrino energy satisfies

$$\sqrt{2} G_F N_e \mp \frac{\Delta m^2}{2E} \cos 2\theta = 0 \quad \Rightarrow \quad \sin^2 2\tilde{\theta} = 1 \quad \Delta \tilde{m}^2 = \Delta m^2 \sin 2\theta. \quad (55)$$

The oscillation amplitude is therefore maximal independently of the value of the vacuum mixing angle.

We also note that

- oscillations vanish at $\theta = 0$, because the oscillation length becomes infinite for $\theta = 0$;
- the resonance is only there for ν or $\bar{\nu}$ but not both;
- the resonance condition depends on the sign($\Delta m^2 \cos 2\theta$):
 - resonance observed in $\nu \rightarrow \text{sign}(\Delta m^2 \cos 2\theta) > 0$,
 - resonance observed in $\bar{\nu} \rightarrow \text{sign}(\Delta m^2 \cos 2\theta) < 0$.

3.3 Neutrino oscillations in variable matter

In the Sun the density of electrons is not constant. However, if the variation is sufficiently slow, the eigenstates of H_{eff} change slowly with the density and we can assume that the neutrino produced in a local eigenstate remains in the same eigenstate along the trajectory. This is the so-called *adiabatic approximation*.

Let us suppose that neutrinos are crossing the Sun. We consider here two-family mixing for simplicity. At any point in the trajectory, it is possible to diagonalize the Hamiltonian fixing the matter density to that at the given point. The resulting eigenstates can be written as

$$|\tilde{\nu}_1\rangle = |\nu_e\rangle \cos \tilde{\theta} - |\nu_\mu\rangle \sin \tilde{\theta}, \quad (56)$$

$$|\tilde{\nu}_2\rangle = |\nu_e\rangle \sin \tilde{\theta} + |\nu_\mu\rangle \cos \tilde{\theta}. \quad (57)$$

Neutrinos are produced close to the centre $x = 0$ where the electron density, $N_e(0)$, is very large. Let us suppose that it satisfies

$$2\sqrt{2}G_F N_e(0) \gg \Delta m^2 \cos 2\theta. \quad (58)$$

Then the diagonalization of the mass matrix at this point gives

$$\tilde{\theta} \simeq \frac{\pi}{2} \Rightarrow |\nu_e\rangle \simeq |\tilde{\nu}_2\rangle \quad (59)$$

in such a way that an electron neutrino is mostly the second mass eigenstate. When neutrinos exit the Sun, at $x = R_\odot$, the matter density falls to zero, $N_e(R_\odot) = 0$, and the local effective mixing angle is the one in vacuum, $\tilde{\theta} = \theta$. If θ is small, the eigenstate $\tilde{\nu}_2$ is mostly ν_μ according to Eq. (57).

Therefore an electron neutrino produced at $x = 0$ is mostly the eigenstate $\tilde{\nu}_2$, but this eigenstate outside the Sun is mostly ν_μ . There is maximum $\nu_e \rightarrow \nu_\mu$ conversion if the adiabatic approximation is a good one. This is the famous MSW effect [13, 14]. The evolution of the eigenstates is shown in Fig. 13: the MSW effect would occur when there is a level crossing in the absence of mixing. The conditions for this to happen are:

- *Resonant condition*: the density at the production is above the critical one

$$N_e(0) > \frac{\Delta m^2 \cos 2\theta}{2\sqrt{2}EG_F}. \quad (60)$$

- *Adiabaticity*: the splitting of the levels is large compared to energy injected in the system by the variation of $N_e(r)$. A measurement of this is given by γ which should be much larger than one:

$$\gamma = \frac{\sin^2 2\theta}{\cos 2\theta} \frac{\Delta m^2}{2E} \frac{1}{|\nabla \log N_e(r)|} > \gamma_{\min} > 1, \quad (61)$$

where $\nabla = \partial/\partial r$.

At fixed energy both conditions give the famous MSW triangles, if plotted on the plane $(\log(\sin^2 2\theta), \log(\Delta m^2))$:

$$\log(\Delta m^2) < \log\left(\frac{2\sqrt{2}G_F N_e(0)E}{\cos 2\theta}\right) \quad (62)$$

$$\log(\Delta m^2) > \log\left(\gamma_{\min} 2E \nabla \log N_e \frac{\cos 2\theta}{\sin^2 2\theta}\right). \quad (63)$$

For example, taking $N_e(r) = N_c \exp(-r/R_0)$, $R_0 = R_\odot/10.54$, $N_c = 1.6 \times 10^{26} \text{ cm}^{-3}$, $E = 1 \text{ MeV}$, these curves are shown in Fig. 14.

As we shall see, the deficit of electron neutrinos coming from the Sun has been interpreted in terms of an MSW effect in neutrino propagation in the Sun. Before the recent experiments SNO and KamLAND that we shall discuss in Section 4.1, there were several solutions possible inside the expected MSW triangle: SMA, LMA and LOW as shown in Fig. 15. The famous SMA and LOW solutions are now history.

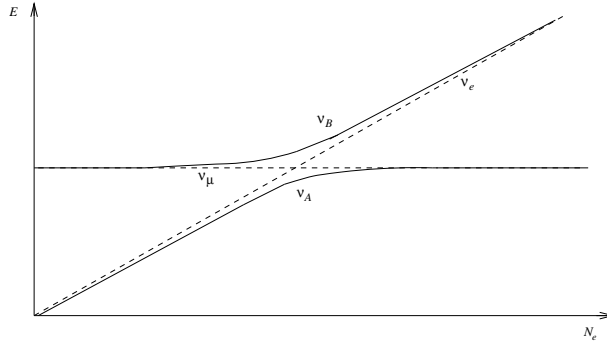


Fig. 13: Evolution of the eigenstates as a function of the distance to the centre of the Sun

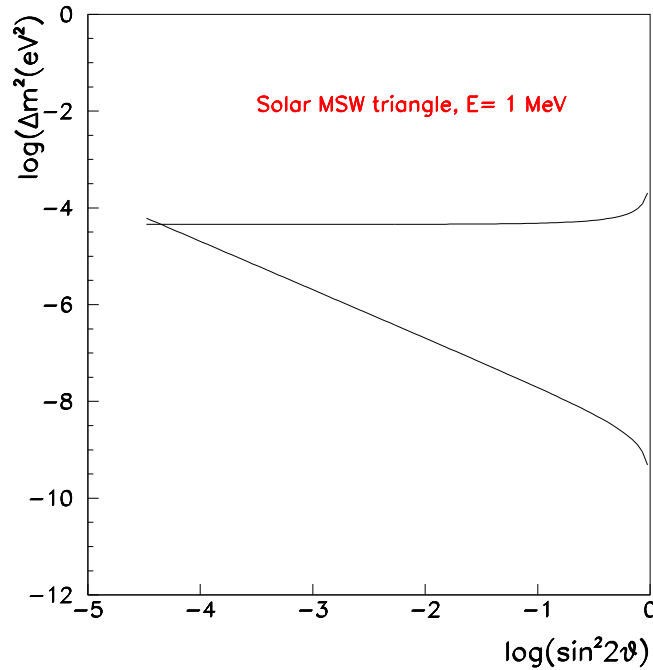


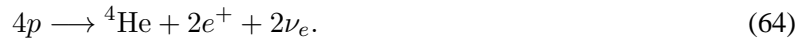
Fig. 14: MSW triangle: in the region between the two lines the resonance and adiabaticity conditions are both satisfied for neutrinos of energy 1 MeV

4 Evidence for neutrino oscillations

Nature has been kind enough to provide us with two natural sources of neutrinos (the Sun and the atmosphere) where neutrino flavour transitions have been observed in a series of ingenious experiments, that started back in the 1960s with the pioneering experiment of R. Davies. This effort has already been rewarded once with the Nobel prize of 2002.

4.1 The solar puzzle

The Sun is an intense source of neutrinos produced in the chain of nuclear reactions that burn hydrogen into helium:



The expected spectral flux of ν_e in the absence of oscillations is shown in Fig. 16. The prediction of this flux obtained by J. Bahcall and collaborators [16] is the result of a detailed simulation of the solar

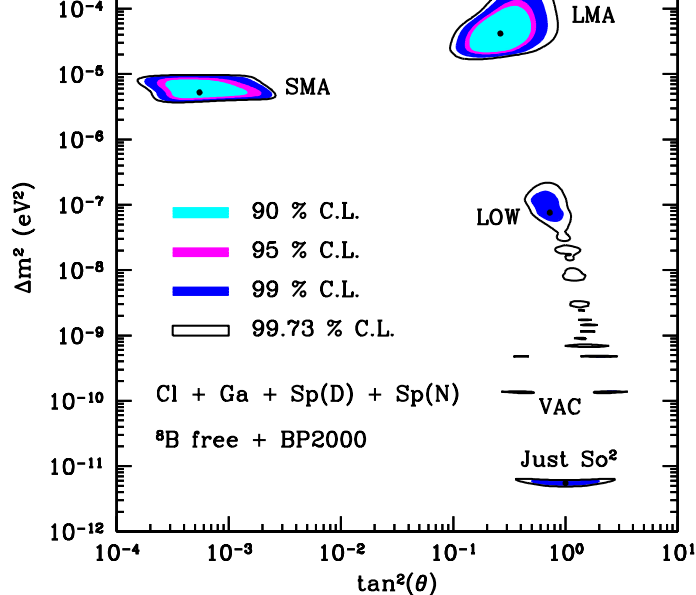


Fig. 15: Neutrino oscillation solutions to the solar neutrino deficit in year 2000 (taken from Ref. [15])

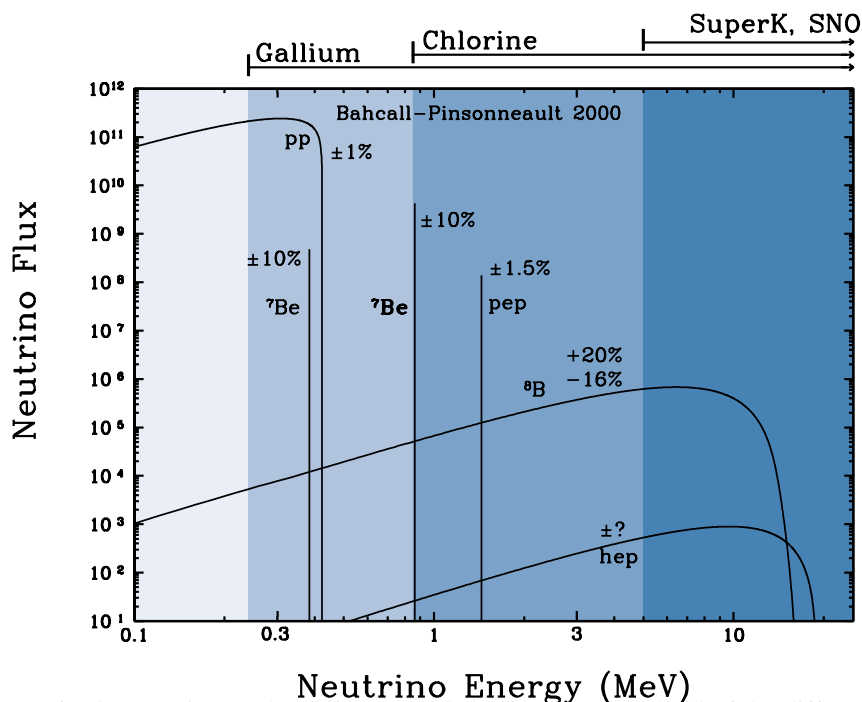


Fig. 16: Spectrum of solar neutrinos. The different bands indicate the threshold of the different detection techniques.

interior and has been improved over many years. It is the so-called standard solar model (SSM).

Neutrinos coming from the Sun have been detected with several experimental techniques that have a different neutrino energy threshold as indicated in Fig. 16. On the one hand, the radiochemical techniques, used in the experiments Homestake (chlorine, ^{37}Cl) [17], Gallex/GNO [18] and Sage [19] (using gallium, ^{71}Ga , and germanium, ^{71}Ge , respectively), can count the total number of neutrinos with a rather low threshold ($E_\nu > 0.81$ MeV in Homestake and $E_\nu > 0.23$ MeV in Gallex and Sage), they cannot get any information on the directionality, the energy of the neutrinos, nor the time of the event. On the other hand, Kamiokande [20] pioneered a new technique to observe solar neutrinos using water Cherenkov detectors. The signal comes from elastic neutrino scattering on electrons (ES), $\nu_e + e^- \rightarrow \nu_e + e^-$, that can be observed from the Cherenkov radiation emitted by the recoiling electrons. These are real-time experiments that provide information on the directionality and the energy of the neutrinos by measuring the recoiling electron. Unfortunately, the threshold for these types of experiments is much higher, ≥ 5 MeV. All these experiments have consistently observed a number of solar neutrinos between 1/3 and 1/2 of the number expected in the SSM and for a long time this was referred to as the *solar*

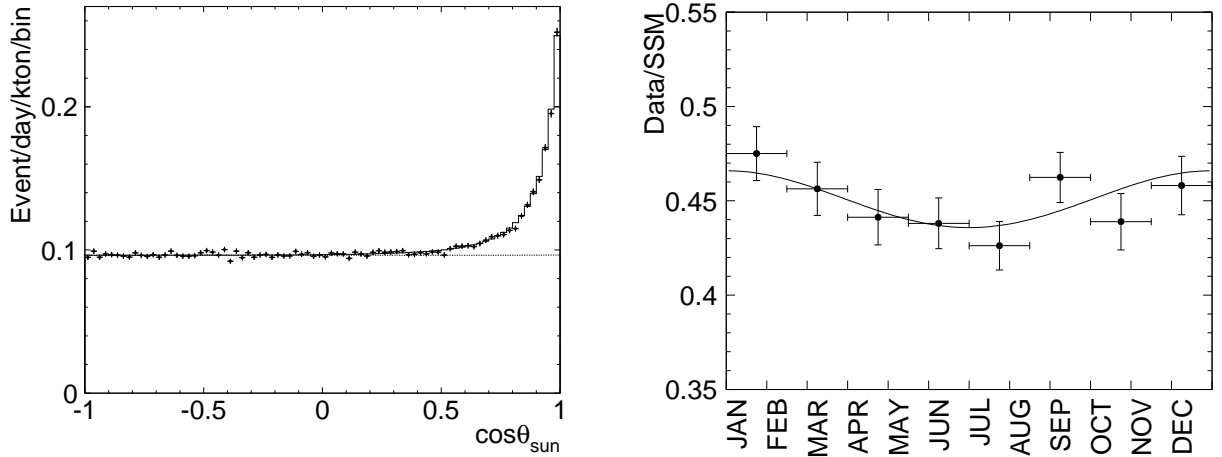


Fig. 17: Left: distribution of solar neutrino events as a function of the zenith angle of the Sun. Right: seasonal variation of the solar neutrino flux in SuperKamiokande.

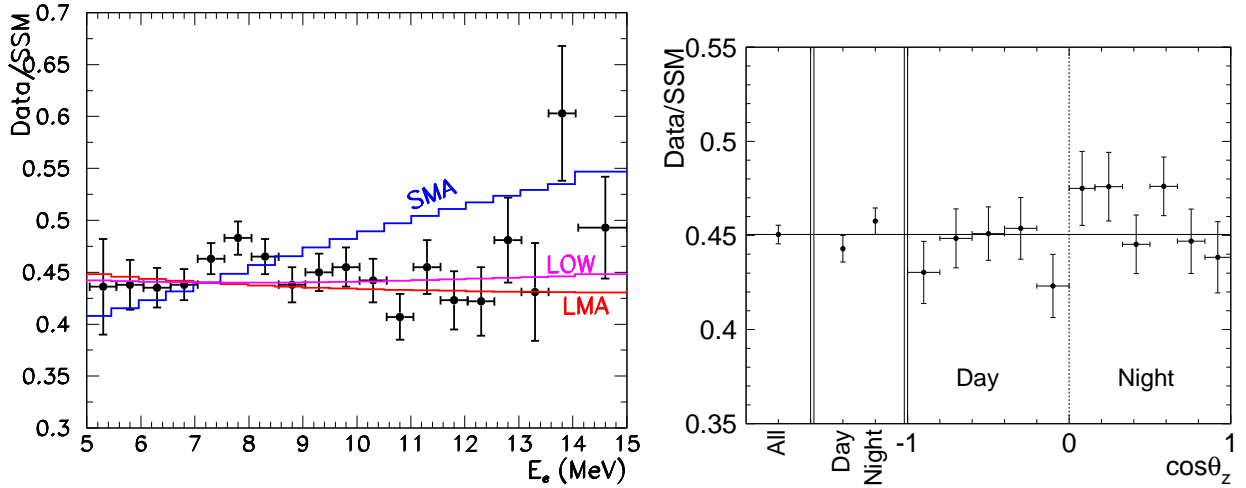


Fig. 18: Left: Distribution of the solar neutrino events as a function of the electron energy. Right: Day–night distribution of the solar neutrino events in SuperKamiokande.

neutrino problem or deficit.

The progress in this field over the past ten years has been enormous culminating in a solution to this puzzle that no longer relies on the predictions of the standard solar model.

There have been three milestones.

1998: SuperKamiokande [21] measured the solar neutrino deficit with unprecedented precision. Furthermore the measurement of the direction of the events demonstrated that the neutrinos measured definitely come from the Sun: the left plot of Fig. 17 shows the distribution of the events as a function of the zenith angle of the Sun. A seasonal variation of the flux is expected since the distance between the Earth and the Sun varies seasonally. The right plot of Fig. 17 shows that the measured variation is in perfect agreement with that expectation. If the deficit of ν_e in the Sun is interpreted in terms of neutrino oscillations, two very important observables to discriminate between different solutions are the spectral distribution of the events shown in the left plot of Fig. 18, which shows a rather flat spectrum, and the day/night asymmetry. The latter is important because neutrinos arriving from the Sun at night have to cross the Earth and some of the possible solutions are such that matter effects in neutrino propagation in the Earth are relevant. The analysis of solar data in year 2000 in terms of neutrino oscillations of the ν_e into some other type indicated a number of possible solutions as shown in Fig. 15.

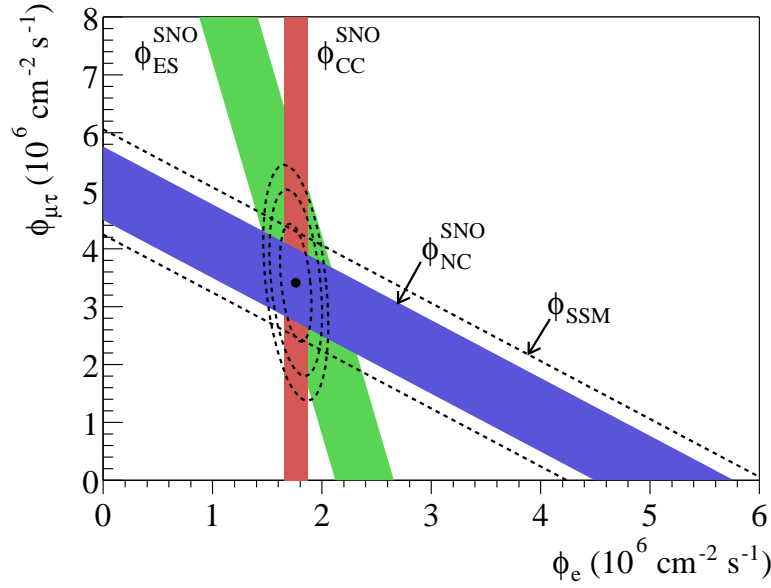


Fig. 19: Flux of ν_μ and ν_τ versus the flux of ν_e in the solar neutrino flux as measured from the three reactions observable in the SNO experiment. The dashed band shows the prediction of the SSM, which agrees perfectly with the flux measured with the NC reaction (from Ref. [23]).

2001: The SNO experiment [22] measured the flux of solar neutrinos using the three reactions:

$$(CC) \quad \nu_e + d \rightarrow p + p + e^- \quad E_{\text{thres}} > 5 \text{ MeV} \quad (65)$$

$$(NC) \quad \nu_x + d \rightarrow p + n + \nu_x \quad x = e, \mu, \tau \quad E_{\text{thres}} > 2.2 \text{ MeV} \quad (66)$$

$$(ES) \quad \nu_e + e^- \rightarrow \nu_e + e^- \quad E_{\text{thres}} > 5 \text{ MeV} \quad (67)$$

Since the CC reaction is only sensitive to electron neutrinos, while the NC one is sensitive to all the types that couple to the Z^0 boson, the comparison of the fluxes measured with both reactions can establish if there are ν_μ and ν_τ in the solar flux independently of the normalization given by the SSM. The neutrino fluxes measured by the three reactions by SNO are:

$$\phi^{\text{CC}} = 1.67(9) \times 10^6 \text{ cm}^{-2}\text{s}^{-1}, \quad \phi^{\text{NC}} = 5.54(48) \times 10^6 \text{ cm}^{-2}\text{s}^{-1}, \quad \phi^{\text{ES}} = 1.77(26) \times 10^6 \text{ cm}^{-2}\text{s}^{-1}. \quad (68)$$

These measurements demonstrate that the Sun shines (ν_μ, ν_τ) about two times more than it shines ν_e , which constitutes the first direct demonstration of flavour transitions in the solar flux! Furthermore the NC flux that measures all active species in the solar flux, is compatible with the total ν_e flux expected according to the SSM as shown in Fig. 19.

The post-SNO global fits of all solar data shown in Fig. 20 (left) in terms of neutrino oscillations are quite different from those in Fig. 15. Of all the possible solutions, only the one at the largest mixing angle and mass square difference survives, the famous LMA solution.

2002: The solar oscillation is confirmed with reactor neutrinos in the KamLAND experiment [24]. This is 1kton of liquid scintillator which measures the flux of reactor neutrinos produced in a cluster of nuclear plants around Kamioka. The average distance is $\langle L \rangle = 175 \text{ km}$. Neutrinos are detected via inverse β -decay which has a threshold energy of about 2.6 MeV:

$$\bar{\nu}_e + p \rightarrow e^+ + n \quad E_{\text{th}} > 2.6 \text{ MeV} . \quad (69)$$

The fortunate circumstance that

$$\langle E_\nu(1 \text{ MeV}) \rangle / L(100 \text{ km}) \sim 10^{-5} \text{ eV}^2 \quad (70)$$

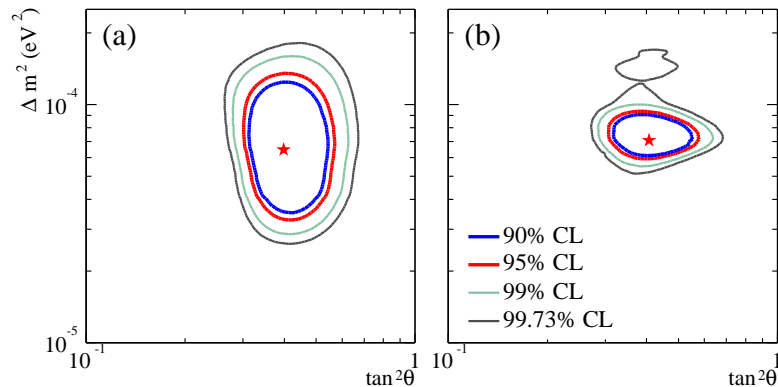


Fig. 20: Left: Analysis of all solar data in terms of neutrino oscillations. Right: Analysis including also KamLAND data (from Ref. [22]).

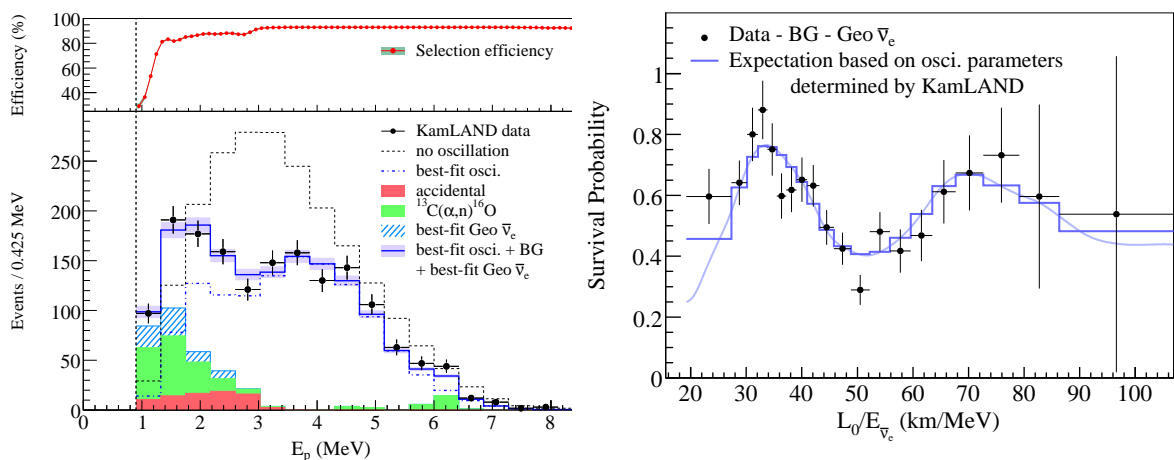


Fig. 21: Spectral distribution of the $\bar{\nu}_e$ events in KamLAND (left) and E_ν/L dependence (right). The data are compared to the expectation in the absence of oscillations and to the best fit oscillation hypothesis (from Ref. [25]).

is in the range indicated by solar data, and that the expected mixing angle is large, implies that a large depletion of the expected antineutrino flux (which is known to a few per cent accuracy) should be observed together with a significant energy dependence.

Figure 21 shows the latest KamLAND results [25] for the spectral distribution of events as well as as a function of the ratio E_ν/L . They have recently lowered the energy threshold and have sensitivity to geoneutrinos. The measurements of geoneutrinos could have important implications in geophysics. Concerning the sensitivity to the oscillation parameters, Fig. 22 shows the present determination of the solar oscillation parameters from KamLAND and other solar experiments. The precision in the determination of $\Delta m_{\text{solar}}^2$ is spectacular and shows that neutrino experiments are entering the era of precision physics.

Last year new data was presented by a new solar neutrino experiment Borexino [26]. It is the lowest-threshold real-time solar neutrino experiment and the only one that could measure the flux of the monochromatic ${}^7\text{Be}$ neutrinos:

$$\Phi({}^7\text{Be}) = 5.08(25) \times 10^9 \text{ cm}^{-2}\text{s}^{-1} .$$

The relevance of Borexino is illustrated in Fig. 23. The result is in agreement with the oscillation interpretation of other solar and reactor experiments and it adds further information to disfavour alternative exotic interpretations of the data.

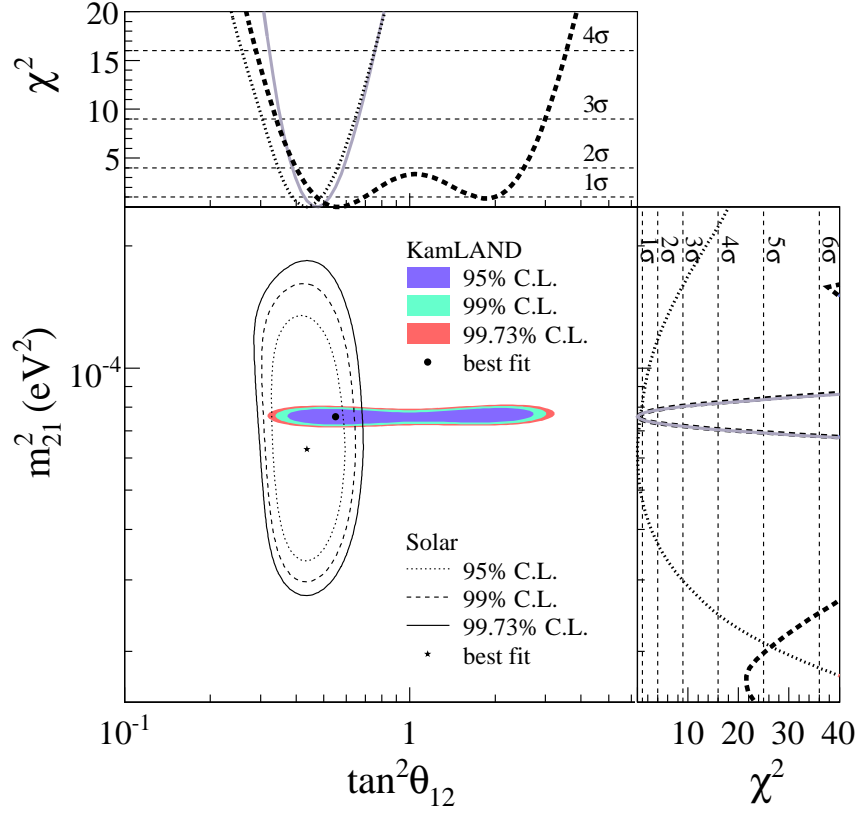


Fig. 22: Analysis of all solar and KamLAND data in terms of oscillations (from Ref. [25])

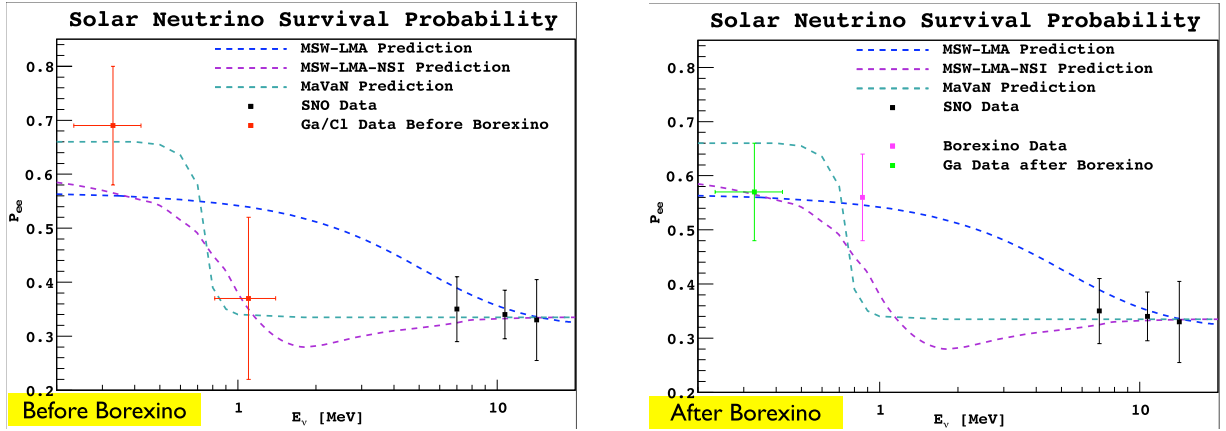


Fig. 23: Comparison of solar neutrino fluxes measured by the different experiments before Borexino (left) and after (right). Presented by the Borexino Collaboration at Neutrino 2008.

In summary, solar neutrinos experiments have made fundamental discoveries in particle physics and are now becoming useful for other applications, such as a precise understanding of the Sun and the Earth.

4.2 Atmospheric neutrino anomaly

Neutrinos are also produced in the atmosphere when primary cosmic rays impinge on it producing K, π that subsequently decay. The fluxes of such neutrinos can be predicted within a 10–20% accuracy to be those in the left plot of Fig. 24.

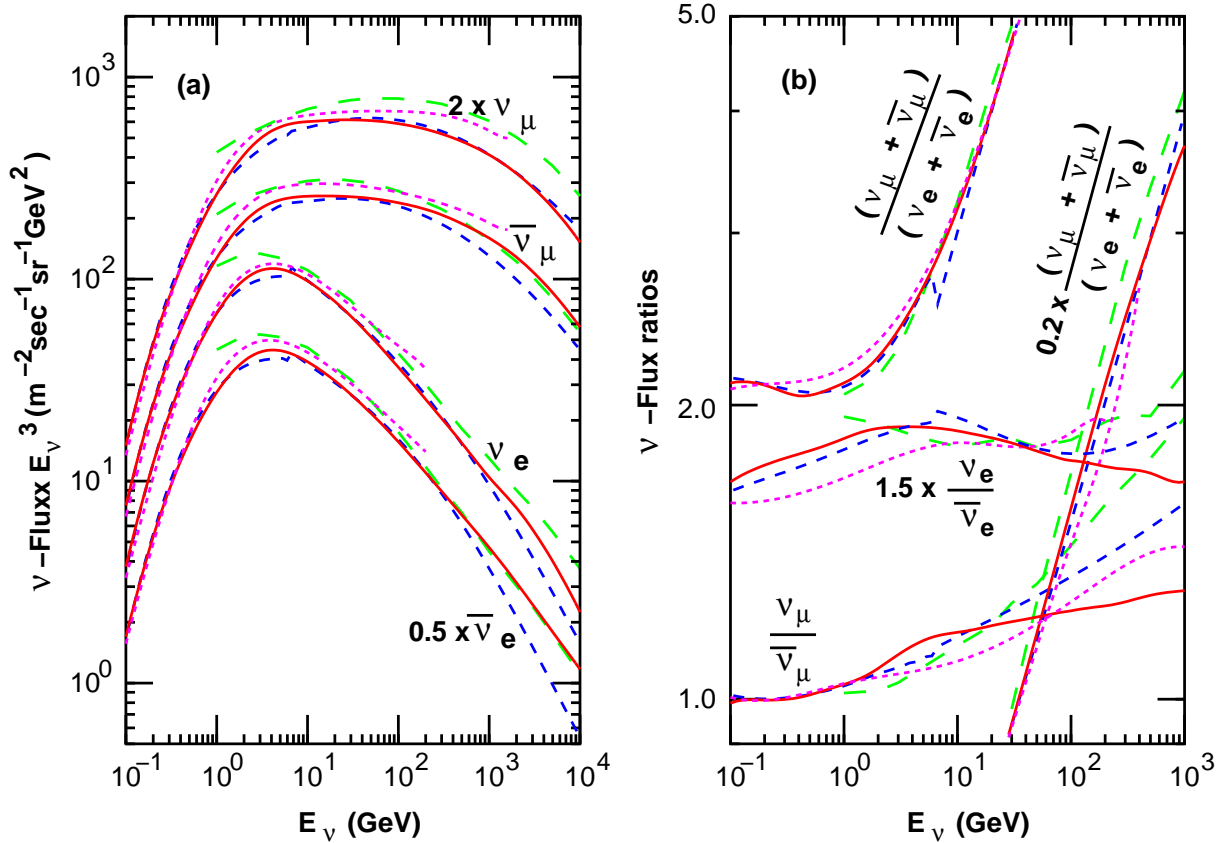


Fig. 24: Comparison of the predictions of different Monte Carlo simulations of the atmospheric neutrino fluxes averaged over all directions (left) and of the flux ratios $(\nu_\mu + \bar{\nu}_\mu)/(\nu_e + \bar{\nu}_e)$, $\nu_\mu/\bar{\nu}_\mu$, and $\nu_e/\bar{\nu}_e$ (right). The solid line corresponds to a recent full 3D simulation. Taken from the last reference in Ref. [27].

Clearly, atmospheric neutrinos are an ideal place to look for neutrino oscillation since the E_ν/L span several orders of magnitude, with neutrino energies varying from a few hundred MeV to 10^3 GeV and distances between production and detection varying from 10 – 10^4 km, as shown in Fig. 25 (right).

Many of the uncertainties in the predicted fluxes cancel when the ratio of muon to electron events is considered. The first indication of a problem was found when a deficit was observed precisely in this ratio by several experiments: Kamiokande [28], IMB [29], Soudan2 [30], Macro [31].

In 1998, SuperKamiokande clarified to a large extent the origin of this anomaly [32]. This experiment can distinguish muon and electron events, measure the direction of the outgoing lepton (the zenith angle with respect to the Earth's axis) which is correlated to that of the neutrino (the higher the energy the higher the correlation), in such a way that they could measure the variation of the flux as a function of the distance travelled by the neutrinos. Furthermore, they considered different samples of events: sub-GeV (lepton with energy below 1 GeV), multi-GeV (lepton with energy above 1 GeV), together with stopping and through-going muons that are produced on the rock surrounding Superkamiokande. The different samples correspond to different parent neutrino energies as can be seen in Fig. 25 (left). The number of events for the different samples as a function of the zenith angle of the lepton are shown in Fig. 26.

While the electron events observed are in agreement with predictions, a large deficit of muon events was found with a strong dependence on the zenith angle: the deficit was almost 50% for those events corresponding to neutrinos coming from below $\cos\theta = -1$, while there is no deficit for those coming from above. The quality of the fit to the neutrino oscillation hypothesis $\nu_\mu \rightarrow \nu_\tau$ is shown in the plot. The perfect fit to the oscillation hypothesis is rather non-trivial given the sensitivity of this

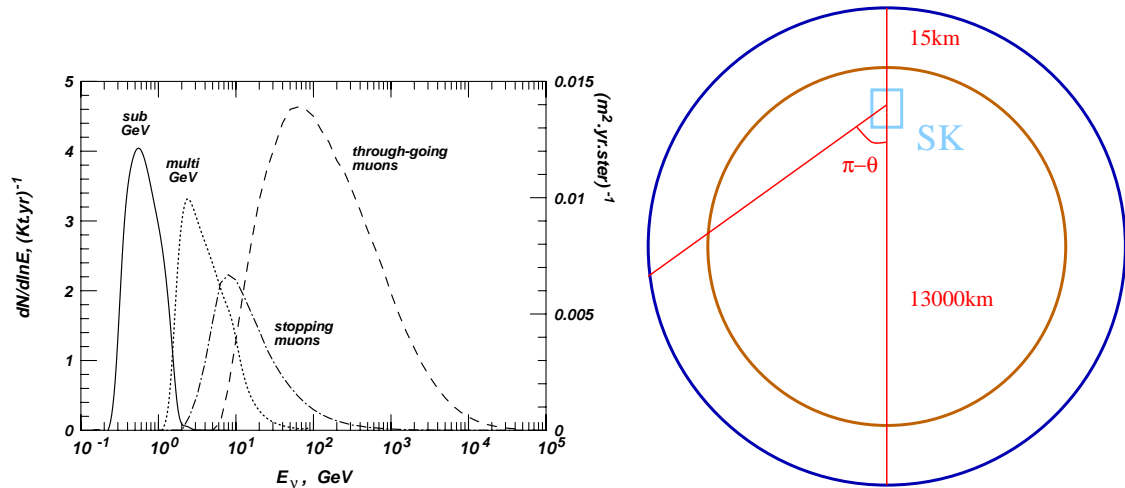


Fig. 25: Left: Parent neutrino energies of the different samples considered in Superkamiokande: sub-GeV, multi-GeV, stopping and through-going muons. Right: Distances travelled by atmospheric neutrinos as a function of the zenith angle.

measurement to the E_ν (different samples) and L (zenith angle) dependence. The significance of the E_ν/L dependence has been presented recently by the SuperKamiokande Collaboration [34], as shown in Fig. 27.

Appropriate neutrino beams to search for the atmospheric oscillation can easily be produced at accelerators if the detector is located at a long baseline of a few hundred kilometres, since

$$|\Delta m_{\text{atmos}}^2| \sim \frac{E_\nu(1 - 10 \text{ GeV})}{L(10^2 - 10^3 \text{ km})}. \quad (71)$$

A *conventional* neutrino beam is produced from protons hitting a target and producing π and K :

$$p \rightarrow \text{Target} \rightarrow \pi^+, K^+ \rightarrow \nu_\mu (\% \nu_e, \bar{\nu}_\mu, \bar{\nu}_e) \quad (72)$$

$$\nu_\mu \rightarrow \nu_x. \quad (73)$$

Those of a selected charge are focused and are left to decay in a long decay tunnel producing a neutrino beam of mostly muon neutrinos (or antineutrinos) with a contamination of electron neutrinos of a few per cent. The atmospheric oscillation can be established by studying, as a function of the energy, either the disappearance of muon neutrinos or, if the energy of the beam is large enough, the appearance of τ neutrinos.

There are three such conventional beams: KEK–Kamioka ($L = 235$ km), Fermilab–Soudan ($L = 730$ km), CERN–Gran Sasso ($L = 730$ km). The latter being the only one sensitive to ν_τ appearance. The K2K experiment at Kamioka has already presented a positive signal for ν_μ disappearance [35], confirming the atmospheric oscillation. Their result is shown in Fig. 28. More recently also the MINOS experiment has presented a positive result as shown in Fig. 29.

4.3 Reactor experiments in the atmospheric range

Experiments that look for the disappearance of reactor $\bar{\nu}_e$ at an $E_\nu/L \sim \Delta m_{\text{atmos}}^2$ have also been performed [36–38]. The most sensitive of these has been Chooz [38]. No disappearance of $\bar{\nu}_e$ was observed, which excludes the parameter range shown in Fig. 30. Although SuperKamiokande had already established that atmospheric $\nu_e/\bar{\nu}_e$ do not seem to oscillate in the atmospheric range, the sensitivity of SuperKamiokande to this oscillation turns out to be much worse than that of Chooz because of the presence of electron and muon neutrinos in the atmospheric flux. It is in the context of three-neutrino mixing that the negative signal of Chooz has been most relevant, as we shall see.

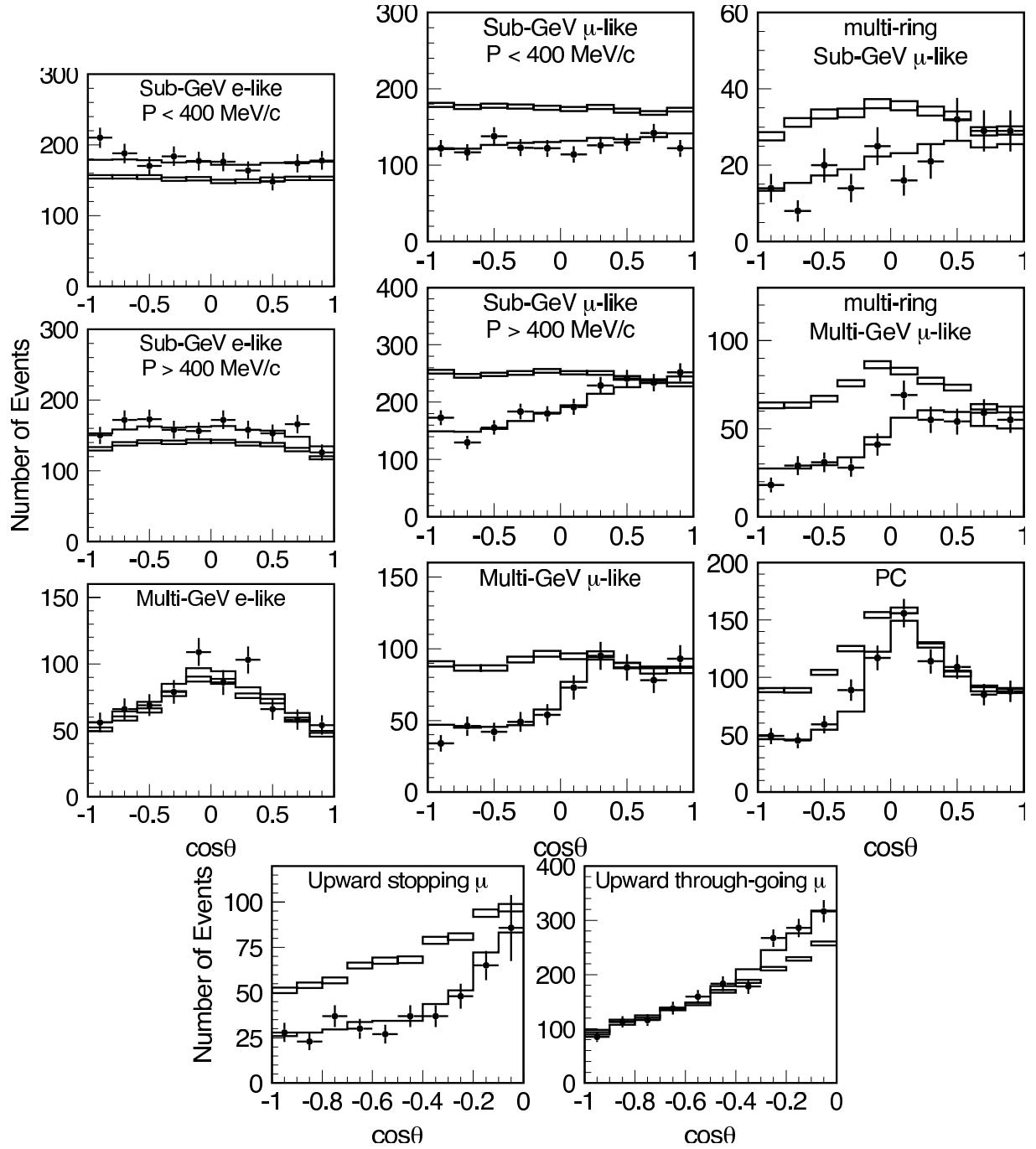


Fig. 26: Zenith angle distribution for fully-contained single-ring e -like and μ -like events, multi-ring μ -like events, partially contained events, and upward-going muons. The points show the data and the solid lines show the Monte Carlo events without neutrino oscillation. The dashed lines show the best-fit expectations for $\nu_\mu \leftrightarrow \nu_\tau$ oscillations (from Ref. [33]).

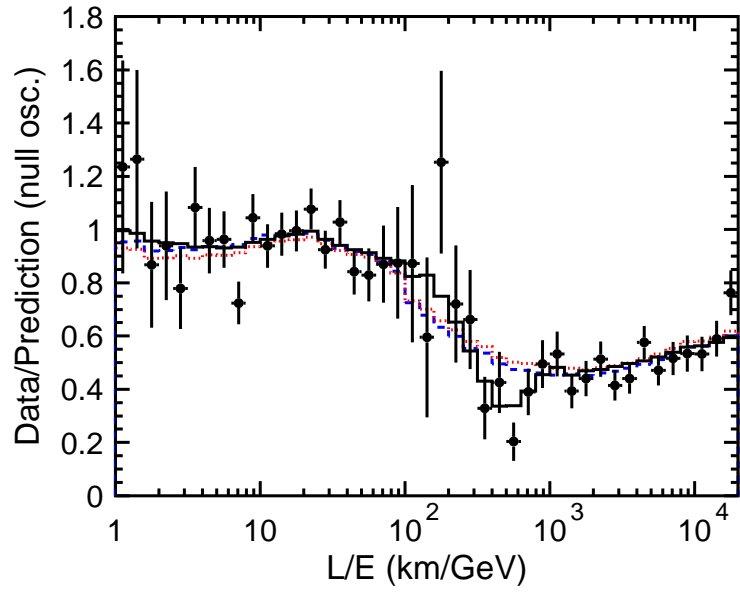


Fig. 27: Ratio of the data to the non-oscillated Monte Carlo events (points) with the best-fit expectation for 2-flavour $\nu_\mu \leftrightarrow \nu_\tau$ oscillations (solid line) as a function of E_ν/L (from Ref. [34]).

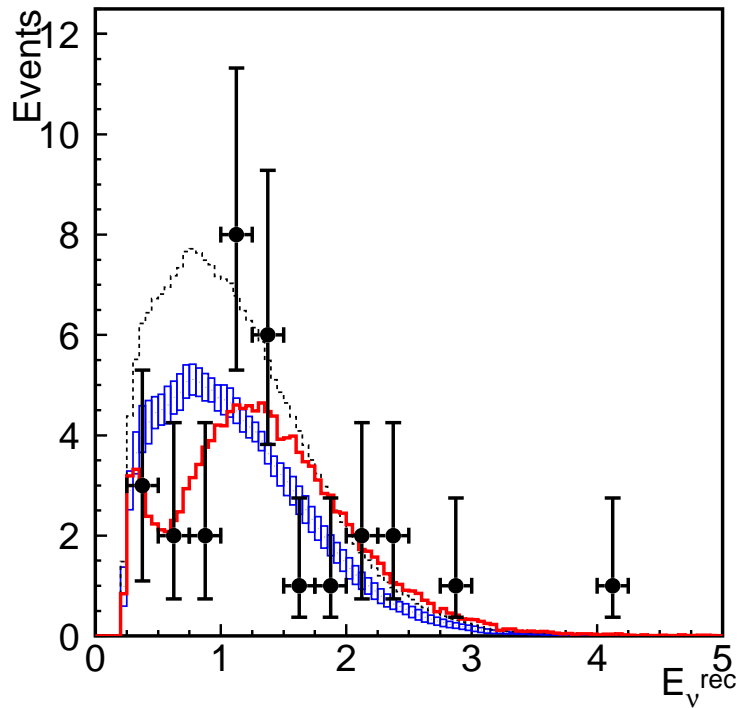


Fig. 28: Distribution of ν_μ events in K2K as a function of the *reconstructed* neutrino energy (from Ref. [35])

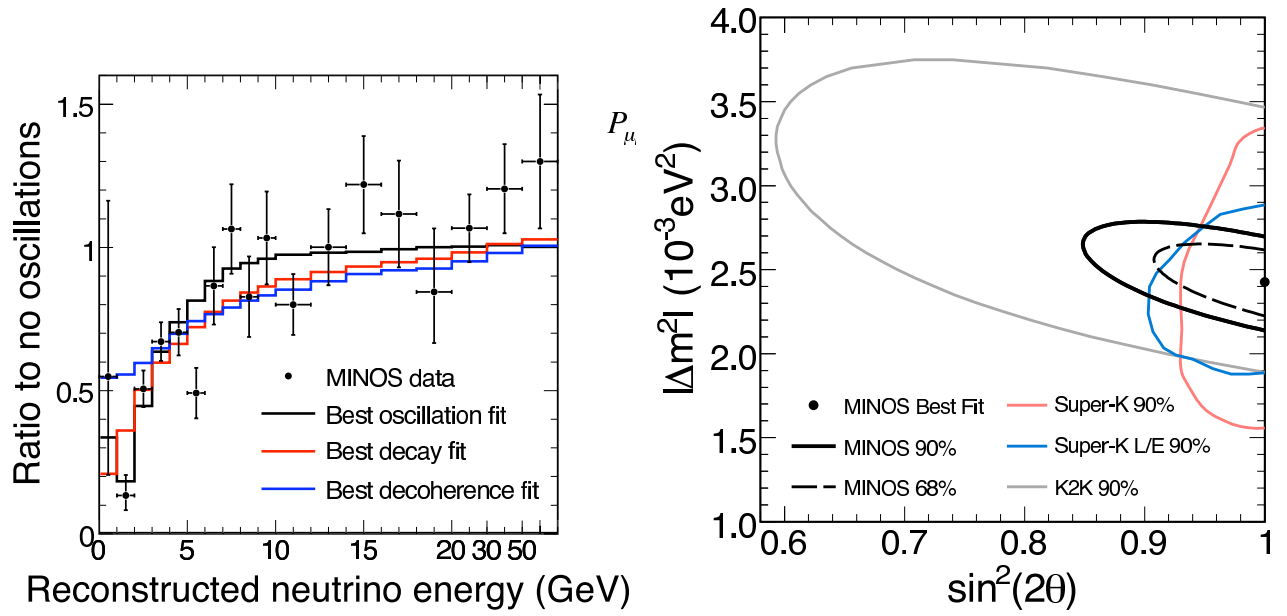


Fig. 29: Left: Ratio of measured to expected (in absence of oscillations) neutrino events in MINOS as a functions of neutrino energy. Right: Determination of oscillation parameters from MINOS data compared to K2K and Super-K.

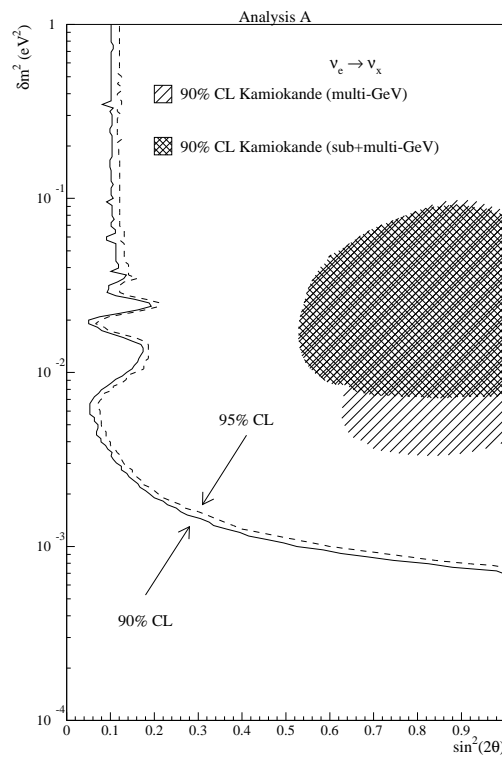


Fig. 30: Range of oscillation parameters for the oscillation $\bar{\nu}_e \rightarrow \bar{\nu}_x$ excluded by the Chooz data (from Ref. [38])

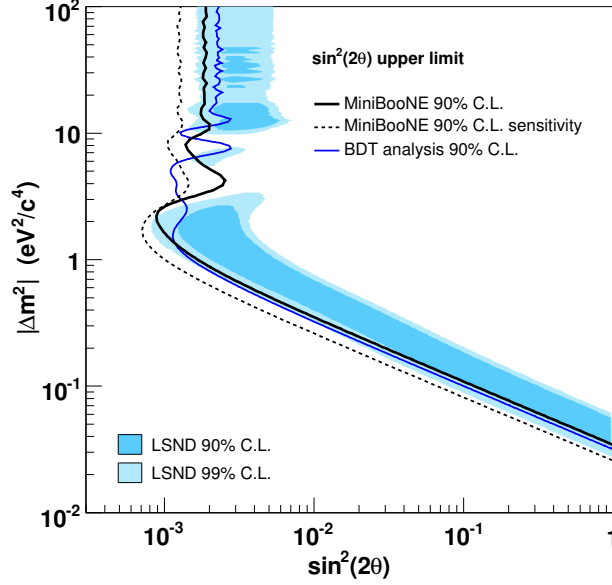


Fig. 31: Range of parameters for the oscillation $\nu_\mu \rightarrow \nu_e$ that could explain LSND data and those excluded by MiniBOONE (from Ref. [41])

4.4 LSND

Finally, an accelerator experiment, LSND, has found an appearance signal that could be interpreted in terms of neutrino flavour transitions [39]. They observed a surplus of electron events in a muon neutrino beam from π^+ decaying in flight (DIF) and a surplus of positron events in a neutrino beam from μ^+ decaying at rest (DAR). The interpretation of this data in terms of neutrino oscillations gives the range shown by a coloured band in Fig. 31:

$$\begin{aligned}
 \pi^+ &\rightarrow \mu^+ \nu_\mu \\
 &\quad \nu_\mu \rightarrow \nu_e \quad \text{DIF } (28 \pm 6/10 \pm 2) \\
 \mu^+ &\rightarrow e^+ \nu_e \bar{\nu}_\mu \\
 &\quad \bar{\nu}_\mu \rightarrow \bar{\nu}_e \quad \text{DAR } (64 \pm 18/12 \pm 3)
 \end{aligned}$$

Part of this region was already excluded by the experiment KARMEN [40] that has unsuccessfully searched for $\bar{\nu}_\mu \rightarrow \bar{\nu}_e$ in a similar range.

In 2006 the first results from MiniBOONE were presented. This experiment was designed to search for $\nu_\mu \rightarrow \nu_e$ transitions in the region of the LSND signal. They did not find confirmation of LSND as shown in Fig. 31

4.5 Three-neutrino mixing

As we have seen there is experimental evidence for neutrino oscillation pointing to three distinct neutrino mass square differences:

$$\underbrace{|\Delta m_{\text{Sun}}^2|}_{\sim 8 \cdot 10^{-5} \text{ eV}^2} \ll \underbrace{|\Delta m_{\text{atmos}}^2|}_{\sim 2.5 \cdot 10^{-3} \text{ eV}^2} \ll \underbrace{|\Delta m_{\text{LSND}}^2|}_{> 0.1 \text{ eV}^2} \quad (74)$$

Clearly the mixing of the three standard neutrinos ν_e, ν_μ, ν_τ can only explain two of the anomalies, so the explanation of the three sets of data would require the existence of a sterile ν species, since only three light neutrinos can couple to the Z^0 boson.

The existence of extra light sterile neutrinos could accommodate a third splitting, but all such scenarios give a very poor fit to all data.

It is now the standard scenario to consider three-neutrino mixing dropping the LSND result. The two independent neutrino mass square differences are assigned to the solar and atmospheric ones:

$$\Delta m_{13}^2 = m_3^2 - m_1^2 = \Delta m_{\text{atmos}}^2, \quad \Delta m_{12}^2 = m_2^2 - m_1^2 = \Delta m_{\text{Sun}}^2. \quad (75)$$

With this convention, the mixing angles θ_{23} and θ_{12} in the parametrization of Eq. (28) correspond approximately to the ones measured in atmospheric and solar oscillations, respectively. This is because solar and atmospheric anomalies approximately decouple as independent 2-by-2 mixing phenomena thanks to the hierarchy between the two mass splittings, $|\Delta m_{\text{atmos}}^2| \gg |\Delta m_{\text{Sun}}^2|$, on the one hand and the fact that the angle θ_{13} , which measures the electron component of the third mass eigenstate element $\sin \theta_{13} = (V_{\text{MNS}})_{e3}$, is small.

To see this, let us first consider the situation in which $E_\nu/L \sim \Delta m_{13}^2$. We can thus neglect the solar mass square difference in front of the atmospheric one and E_ν/L . The oscillation probabilities obtained in this limit are given by

$$P(\nu_e \rightarrow \nu_\mu) \simeq s_{23}^2 \sin^2 2\theta_{13} \sin^2 \left(\frac{\Delta m_{13}^2 L}{4E_\nu} \right), \quad (76)$$

$$P(\nu_e \rightarrow \nu_\tau) \simeq c_{23}^2 \sin^2 2\theta_{13} \sin^2 \left(\frac{\Delta m_{13}^2 L}{4E_\nu} \right), \quad (77)$$

$$P(\nu_\mu \rightarrow \nu_\tau) \simeq c_{13}^4 \sin^2 2\theta_{23} \sin^2 \left(\frac{\Delta m_{13}^2 L}{4E_\nu} \right). \quad (78)$$

Only two angles enter these formulae: θ_{23} and θ_{13} . The latter is the only one that enters the disappearance probability for ν_e in this regime:

$$P(\nu_e \rightarrow \nu_e) = 1 - P(\nu_e \rightarrow \nu_\mu) - P(\nu_e \rightarrow \nu_\tau) \simeq \sin^2 2\theta_{13} \sin^2 \left(\frac{\Delta m_{13}^2 L}{4E_\nu} \right). \quad (79)$$

This is precisely the measurement of the Chooz experiment. Therefore the result of Chooz constrains the angle θ_{13} to be unobservably small.

If θ_{13} is set to zero in Eq. (78), the only probability that survives is the $\nu_\mu \rightarrow \nu_\tau$ one, which has the same form as a 2-family mixing formula Eq. (40) if we identify

$$(\Delta m_{\text{atmos}}^2, \theta_{\text{atmos}}) \rightarrow (\Delta m_{13}^2, \theta_{23}). \quad (80)$$

Instead if $E_\nu/L \sim \Delta m_{12}^2$, the atmospheric oscillation is too rapid and gets averaged out. The survival probability for electrons in this limit is given by:

$$P(\nu_e \rightarrow \nu_e) \simeq c_{13}^4 \left(1 - \sin^2 2\theta_{12} \sin^2 \left(\frac{\Delta m_{12}^2 L}{4E_\nu} \right) \right) + s_{13}^4. \quad (81)$$

Again it depends only on two angles, θ_{12} and θ_{13} , and in the limit in which the latter is zero, the survival probability measured in solar experiments has the form of two-family mixing if we identify

$$(\Delta m_{\text{Sun}}^2, \theta_{\text{Sun}}) \rightarrow (\Delta m_{12}^2, \theta_{12}). \quad (82)$$

The results that we have shown of solar and atmospheric experiments have been analysed in terms of 2-family mixing. The previous argument indicates that when fits are done in the context of 3-family mixing nothing changes very much, thanks to the strong constrain set by Chooz on θ_{13} .

Figure 32 shows the result of a recent global analysis of all data for the different parameters. The 2σ limits are

$$\theta_{23} = 36.9^\circ - 51.3^\circ \quad \theta_{12} = 32.3^\circ - 37.8^\circ \quad \theta_{13} < 10.3^\circ$$

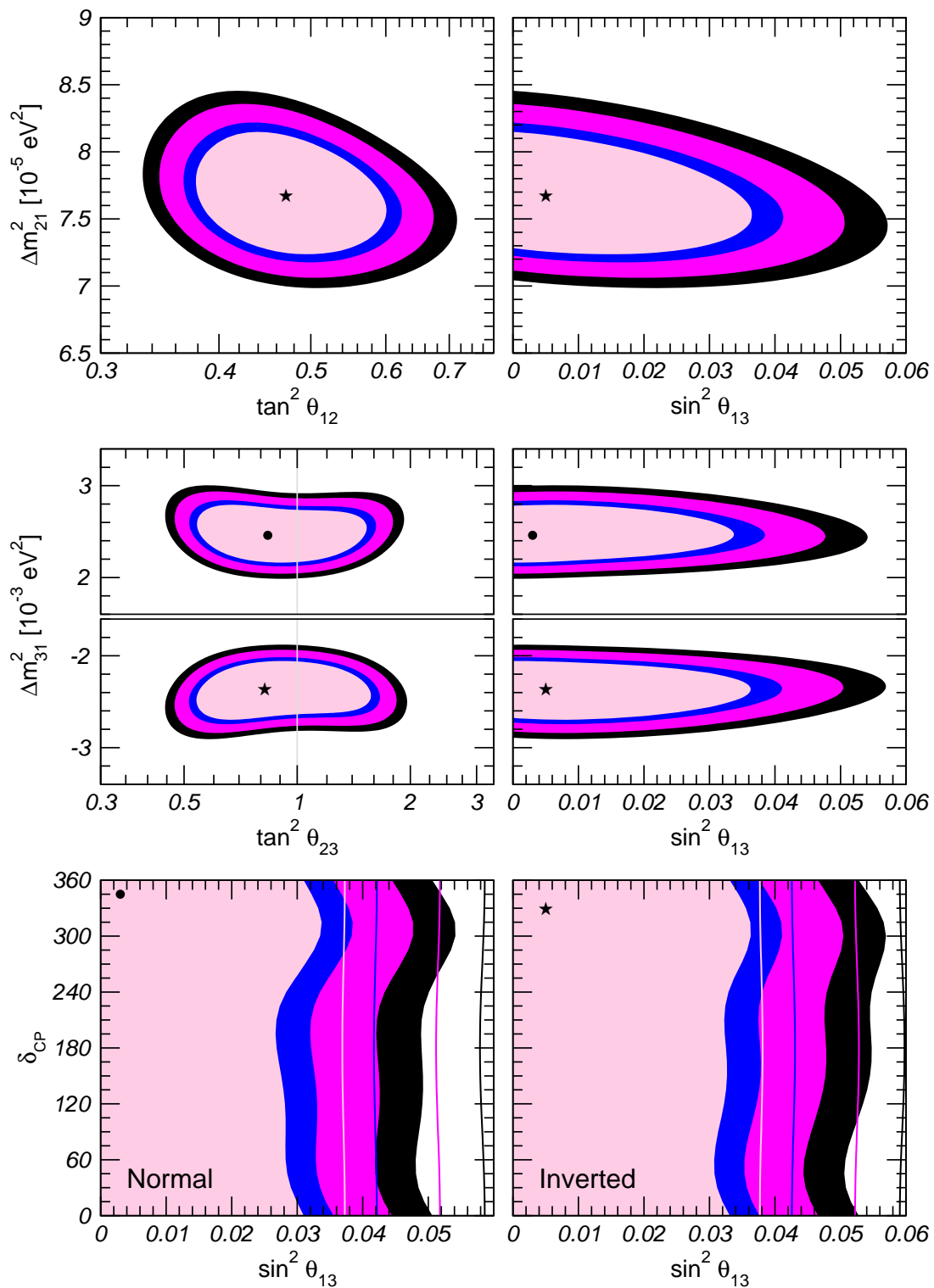


Fig. 32: Fits to the standard 3ν -mixing scenario including all available neutrino oscillation data (from Ref. [42])

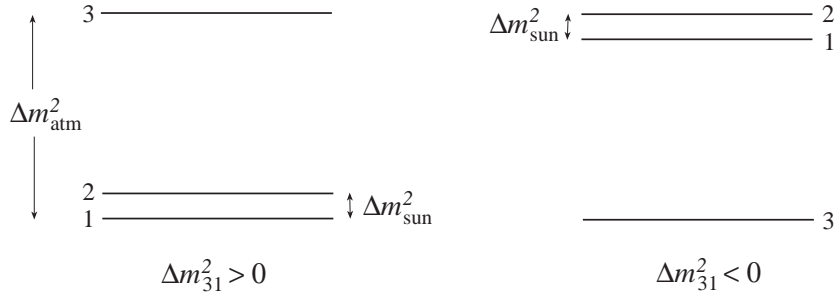


Fig. 33: Possible neutrino spectra consistent with solar and atmospheric data

$$\Delta m_{12}^2 = 7.66(35) \times 10^{-5} \text{ eV}^2 \quad \Delta m_{23}^2 = 2.38(27) \times 10^{-3} \text{ eV}^2. \quad (83)$$

In summary, all the data, except LSND, can be explained if the neutrino spectrum has a structure as shown in Fig. 33. The neutrino mixing matrix is approximately given by

$$|V_{\text{MNS}}| \simeq \begin{pmatrix} 0.77 & -0.86 & 0.5 & -0.63 & 0 & -0.22 \\ 0.22 & -0.56 & 0.44 & -0.73 & 0.57 & -0.80 \\ 0.21 & -0.55 & 0.40 & -0.71 & 0.59 & -0.82 \end{pmatrix}, \quad (84)$$

and we do not know anything about the phases $(\delta, \alpha_1, \alpha_2)$. Note the striking difference between this mixing matrix and the CKM matrix which is approximately diagonal:

$$V_{\text{CKM}} \simeq \begin{pmatrix} 1 & O(\lambda) & O(\lambda^3) \\ O(\lambda) & 1 & O(\lambda^2) \\ O(\lambda^3) & O(\lambda^2) & 1 \end{pmatrix} \quad \lambda \sim 0.2. \quad (85)$$

The main features are

- Large mixing angles, in particular one is close to maximal.
- There is an intriguing near tri-bimaximal mixing pattern

$$V_{\text{tri-bi}} \simeq \begin{pmatrix} \sqrt{\frac{2}{3}} & \sqrt{\frac{1}{3}} & 0 \\ -\sqrt{\frac{1}{6}} & \sqrt{\frac{1}{3}} & \sqrt{\frac{1}{2}} \\ \sqrt{\frac{1}{6}} & -\sqrt{\frac{1}{3}} & \sqrt{\frac{1}{2}} \end{pmatrix}.$$

5 Prospects in neutrino physics

After the next generation of neutrino experiments that are under construction, we shall probably still be far from having complete knowledge of the neutrino mass matrix. There remain several fundamental questions to be answered:

1. Are neutrinos Dirac or Majorana particles?
2. Is total lepton number conserved or violated?
3. What is the absolute neutrino mass scale? Is it a new physics scale?
4. What is the neutrino mass spectrum: i.e., $\Delta m_{\text{atmos}}^2 >$ or < 0 ?
5. Is there CP violation in the lepton sector?
6. What is the value of θ_{13} ?

The best hope addressing the first three questions lies in more precise experiments searching for neutrinoless double- β decay, measuring the end-point of β decay as well as cosmological measurements. Figure 34 shows the present constraints on the combination of parameters that is directly measured in $2\beta 0\nu$ experiments:

$$m_{\beta\beta} \equiv |m_{ee}| = |c_{13}^2(m_1c_{12}^2 + m_2e^{i\alpha_1}s_{12}^2) + m_3e^{i\alpha_2}s_{13}^2|, \quad (86)$$

and in cosmology:

$$\Sigma \equiv m_1 + m_2 + m_3. \quad (87)$$

The cosmological data included in this fit is only that from the cosmic microwave background (CMB).

Note that a lot of information on $m_{\beta\beta}$ is already provided by neutrino oscillation experiments. If the hierarchy is inverse ($m_3 \ll m_1, m_2 \sim \sqrt{|\Delta m_{\text{atmos}}^2|}$), there is a lower bound on $m_{\beta\beta} \geq 10^{-2}$ eV, as shown by the red (I.H.) band. Instead, if the hierarchy is normal $m_3 \sim \sqrt{|\Delta m_{\text{atmos}}^2|} \gg m_1, m_2$, there is no lower bound because neither θ_{13} nor m_1 is bounded from below, as shown by the blue (N.H.) band. The horizontal band shows the controversial claim of a positive signal [10].

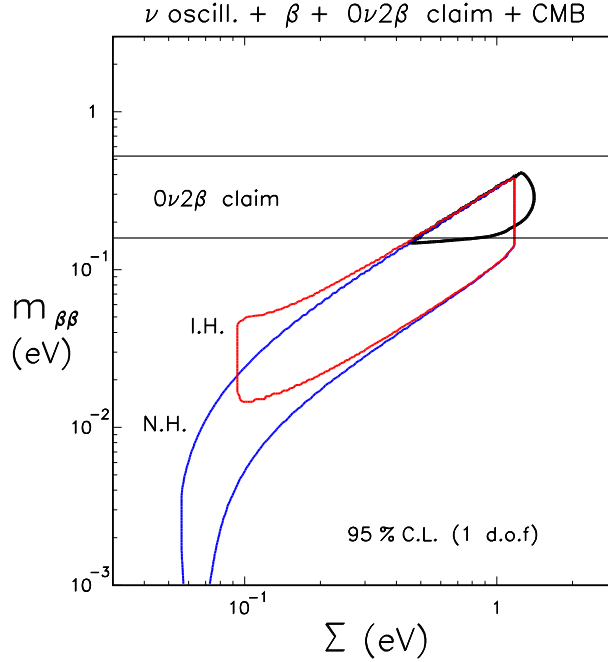


Fig. 34: Present constraints on $m_{\beta\beta}$ and Σ from neutrino experiments and CMB data (from Ref. [43])

A plethora of forthcoming experiments that will improve these constraints are under construction.

KATRIN [44] is an experiment to measure the spectrum of tritium β decay that is expected to improve the sensitivity to the element:

$$m_e \equiv \sqrt{m_1^2 c_{12}^2 c_{13}^2 + m_2^2 s_{12}^2 c_{13}^2 + m_3^2 s_{13}^2} \quad (88)$$

to about 0.2 eV, which is an improvement of one order of magnitude with respect to the present limit in Eq. (6). Concerning $0\nu\beta\beta$ [45] the next step of several experiments using different detector techniques (CUORE, EXO, GENIUS, Majorana, etc.) is to reach the level of precision of $m_{\beta\beta} \sim 0.1$ eV, which would allow testing the positive claim in a definite way. Further in the future there are also proposals to improve this precision by another order of magnitude reaching the 10^{-2} eV level, which could be sufficient to explore the full parameter space in the case of the inverse hierarchy. The measurement of a

non-zero $m_{\beta\beta}$ would not only prove that neutrinos are Majorana and that lepton number is violated, but might give the best determination of the lightest neutrino mass, and even help in establishing the neutrino mass hierarchy.

Concerning cosmology, it is quite impressive that the sensitivity to the neutrino matter component of the Universe has already reached the eV range. Further significant improvements are expected in the near future (e.g., by PLANCK) that can push present limits by at least one order of magnitude.

Concerning the last three fundamental questions above, they can be studied in more precise neutrino oscillation experiments in the atmospheric range (i.e., $\langle E_\nu \rangle / L \sim \Delta m_{\text{atmos}}^2$) optimized to measure the subleading transitions involving ν_e . In particular, $\nu_e \leftrightarrow \nu_\mu$ and $\bar{\nu}_e \leftrightarrow \bar{\nu}_\mu$ are the so-called *golden* measurements [46], while the $\nu_e \leftrightarrow \nu_\tau$ and $\bar{\nu}_e \leftrightarrow \bar{\nu}_\tau$, being experimentally more challenging, are the *silver* ones [47].

5.1 CP violation in neutrino oscillations

As in the quark sector, the mixing matrix of three neutrinos has CP violating phases. The so-called Dirac phase, δ , induces CP violation in neutrino oscillations, that is a difference between $P(\nu_\alpha \rightarrow \nu_\beta)$ and $P(\bar{\nu}_\alpha \rightarrow \bar{\nu}_\beta)$, for $\alpha \neq \beta$. As we saw in the general expression of Eq. (38), CP violation is possible if there are imaginary entries in the mixing matrix that make $\text{Im}[W_{\alpha\beta}^{jk} \equiv [U_{\alpha j} U_{\beta j}^* U_{\alpha k} U_{\beta k}]] \neq 0$. By CPT, disappearance probabilities cannot violate CP however, because under CPT

$$P(\nu_\alpha \rightarrow \nu_\beta) = P(\bar{\nu}_\beta \rightarrow \bar{\nu}_\alpha), \quad (89)$$

so in order to observe a CP or T-odd asymmetry the initial and final flavour must be different, $\alpha \neq \beta$:

$$A_{\alpha\beta}^{CP} \equiv \frac{P(\nu_\alpha \rightarrow \nu_\beta) - P(\bar{\nu}_\alpha \rightarrow \bar{\nu}_\beta)}{P(\nu_\alpha \rightarrow \nu_\beta) + P(\bar{\nu}_\alpha \rightarrow \bar{\nu}_\beta)}, \quad A_{\alpha\beta}^T \equiv \frac{P(\nu_\alpha \rightarrow \nu_\beta) - P(\nu_\beta \rightarrow \nu_\alpha)}{P(\nu_\alpha \rightarrow \nu_\beta) + P(\nu_\beta \rightarrow \nu_\alpha)}. \quad (90)$$

In the case of 3-family mixing it is easy to see that the CP(T)-odd terms in the numerator are the same for all transitions $\alpha \neq \beta$:

$$A_{\nu_\alpha \nu_\beta}^{\text{CP(T)-odd}} = \frac{\overbrace{\sin \delta c_{13} \sin 2\theta_{13} \sin 2\theta_{12} \frac{\Delta m_{12}^2 L}{4E_\nu}}^{\text{solar}} \overbrace{\sin 2\theta_{23} \sin^2 \frac{\Delta m_{13}^2 L}{4E_\nu}}^{\text{atmos}}}{P_{\nu_\alpha \nu_\beta}^{\text{CP-even}}}. \quad (91)$$

As expected, the numerator is GIM suppressed in all the Δm_{ij}^2 and all the angles, because if any of them is zero, the CP-odd phase becomes unphysical.

In order to maximize this asymmetry, it is necessary to perform experiments in the atmospheric range $\langle E_\nu \rangle / L \sim \Delta m_{\text{atmos}}^2$, so that the GIM suppression is minimized. In this case, only two small parameters remain in the CP-odd terms: the solar splitting, Δm_{Sun}^2 (i.e., small compared to the other scales, $\Delta m_{\text{atmos}}^2$ and $\langle E_\nu \rangle / L$), and the angle θ_{13} . The asymmetry is then larger in the subleading transitions: $\nu_e \rightarrow \nu_\mu(\nu_\tau)$, because the CP-even terms in the denominator are also suppressed by the same small parameters. Indeed a convenient approximation for the $\nu_e \leftrightarrow \nu_\mu$ transitions is obtained expanding to second order in both small parameters [46]:

$$\begin{aligned} P_{\nu_e \nu_\mu}(\bar{\nu}_e \bar{\nu}_\mu) &= s_{23}^2 \sin^2 2\theta_{13} \sin^2 \left(\frac{\Delta m_{13}^2 L}{4E_\nu} \right) \equiv P^{\text{atmos}} \\ &+ c_{23}^2 \sin^2 2\theta_{12} \sin^2 \left(\frac{\Delta m_{12}^2 L}{4E_\nu} \right) \equiv P^{\text{solar}} \\ &+ \tilde{J} \cos \left(\pm \delta - \frac{\Delta m_{13}^2 L}{4E_\nu} \right) \frac{\Delta m_{12}^2 L}{4E_\nu} \sin \left(\frac{\Delta m_{13}^2 L}{4E_\nu} \right) \equiv P^{\text{inter}}, \end{aligned} \quad (92)$$

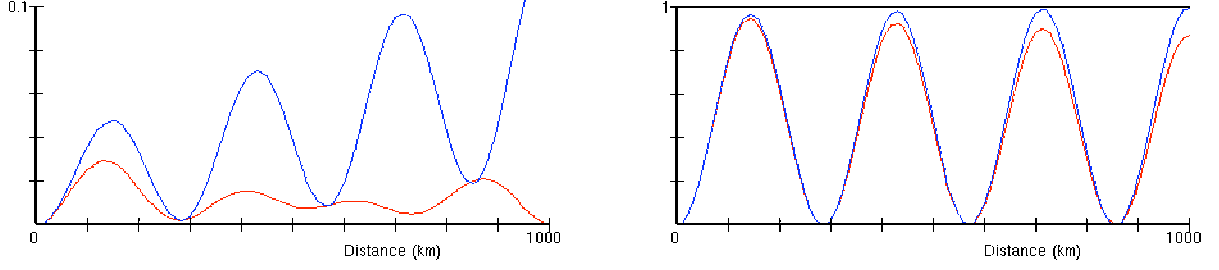


Fig. 35: Comparison of the $\nu_e \leftrightarrow \nu_\mu/\bar{\nu}_e \leftrightarrow \bar{\nu}_\mu$ (left) and $\nu_\mu \leftrightarrow \nu_\tau/\bar{\nu}_\mu \leftrightarrow \bar{\nu}_\tau$ (right) oscillation probabilities for $E_\nu = 500$ MeV, $\theta_{13} = 8^\circ$ and $\delta = 90^\circ$ as a function of the distance

where $\tilde{J} \equiv c_{13} \sin 2\theta_{13} \sin 2\theta_{12} \sin 2\theta_{23}$. This approximate formula is obtained as an expansion to second order in the parameters θ_{13} and Δm_{Sun}^2 . The first term corresponds to the atmospheric oscillation, the second one is the solar one and there is an interference term which has the information on the phase δ . Depending on the value of θ_{13} , it is possible that the atmospheric term dominates over the other two, in such a way that the CP-even terms are suppressed in θ_{13}^2 , or if it is the solar term that dominates, the suppression is in $(\Delta m_{\text{Sun}}^2)^2$. The asymmetries in these two regimes show therefore the following dependence on the small parameters:

$$\begin{aligned}
P^{\text{atmos}} \gg P^{\text{solar}} &\rightarrow A_{\nu_e\nu_\mu(\nu_\tau)}^{CP,T} \sim \frac{\Delta m_{12}^2 L/E_\nu}{\sin 2\theta_{13}}, \\
P^{\text{solar}} \gg P^{\text{atmos}} &\rightarrow A_{\nu_e\nu_\mu(\nu_\tau)}^{CP,T} \sim \frac{\sin 2\theta_{13}}{\Delta m_{12}^2 L/E_\nu}, \\
P^{\text{solar}} \simeq P^{\text{atmos}} &\rightarrow A_{\nu_e\nu_\mu(\nu_\tau)}^{CP,T} = O(1).
\end{aligned} \tag{93}$$

Therefore asymmetries in the subleading transitions are expected to be rather large, specially when the solar and atmospheric terms are comparable.

In contrast, the asymmetries in the leading $\nu_\mu \rightarrow \nu_\tau$ transition in the atmospheric range are much smaller, because the CP-even terms are unsuppressed in each of the two small parameters. The difference between the neutrino and antineutrino oscillation probabilities for the leading and subleading channels are shown in Fig. 35.

5.2 The neutrino spectrum

The oscillation probabilities in matter can also be approximated by an expansion to second order in the two small parameters: θ_{13} and Δm_{12}^2 [46]. The result has the same structure as in vacuum:

$$\begin{aligned}
P_{\nu_e\nu_\mu(\bar{\nu}_e\bar{\nu}_\mu)} &= s_{23}^2 \sin^2 2\theta_{13} \left(\frac{\Delta_{13}}{B_\pm} \right)^2 \sin^2 \left(\frac{B_\pm L}{2} \right) \\
&\quad + c_{23}^2 \sin^2 2\theta_{12} \left(\frac{\Delta_{12}}{A} \right)^2 \sin^2 \left(\frac{AL}{2} \right) \\
&\quad + \tilde{J} \frac{\Delta_{12}}{A} \sin \left(\frac{AL}{2} \right) \frac{\Delta_{13}}{B_\pm} \sin \left(\frac{B_\pm L}{2} \right) \cos \left(\pm\delta - \frac{\Delta_{13} L}{2} \right),
\end{aligned} \tag{94}$$

where

$$B_\pm = |A \pm \Delta_{13}| \quad \Delta_{ij} = \frac{\Delta m_{ij}^2}{2E_\nu} \quad A = \sqrt{2} G_F N_e. \tag{95}$$

This formula shows a resonant enhancement of the atmospheric term in the the neutrino or antineutrino oscillation probability (depending on the sign of Δm_{13}^2) channel when

$$2E_\nu A \sim |\Delta m_{13}^2|. \tag{96}$$

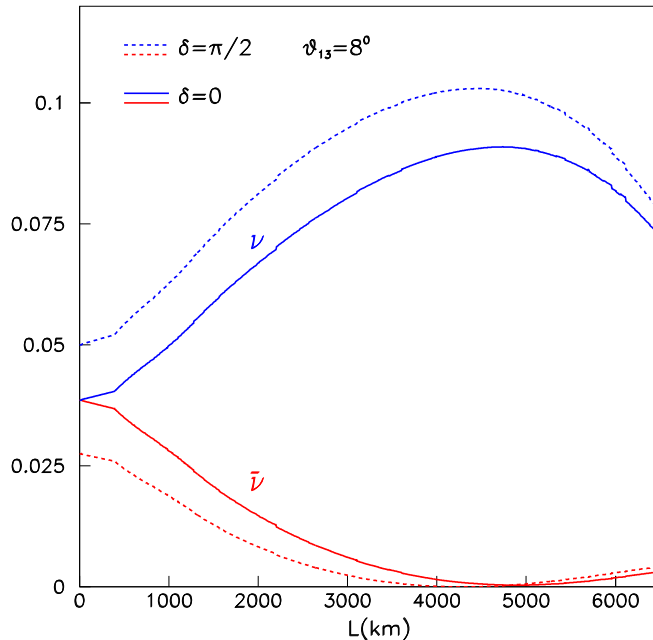


Fig. 36: $P(\nu_e \rightarrow \nu_\mu)$ and $P(\bar{\nu}_e \rightarrow \bar{\nu}_\mu)$ as a function of the baseline L in kilometres, at a neutrino energy $E_\nu/L = |\Delta m_{13}^2|/2\pi$ and for $\theta_{13} = 8^\circ$ and $\delta = 0$ (solid) and 90° (dashed)

Considering the electron number density in the Earth, the resonant energy is $E_\nu \sim 10 - 20$ GeV. This resonance is illustrated in Fig. 36, which shows the $\nu_e \rightarrow \nu_\mu$ oscillation probability for neutrinos and antineutrinos, as a function of the baseline, for neutrino energy constrained to the first atmospheric peak, i.e., $E_\nu/L = |\Delta m_{13}^2|/2\pi$. The difference between the neutrino and anti-neutrino oscillation probabilities induced by matter effects becomes comparable to that due to maximal CP-violation for $L = \mathcal{O}(1000)$ km. This is approximately the baseline where matter effects and CP violation can both be measured simultaneously. At much longer distances, matter effects completely hide CP-violation effects and vice versa.

5.3 The measurement of θ_{13} and δ

5.3.1 Theoretical challenge

In the future, we shall face the challenge of extracting simultaneously θ_{13} , δ and also the hierarchy from the measurement of the oscillation probabilities $\nu_\mu \leftrightarrow \nu_e$ and $\bar{\nu}_\mu \leftrightarrow \bar{\nu}_e$. This turns out to be non-trivial even in principle, because of the existence of degeneracies [48]. In fact, at fixed E_ν, L there are generically two solutions for (θ_{13}, δ) that give the same probabilities for neutrinos and antineutrinos.

This is due to the periodicity in δ : if the equiprobability curves for neutrinos and antineutrinos on the plane (θ_{13}, δ) cross at one point (at the true solution), they must cross at least once more as shown in Fig. 37.

The fake solution has a strong dependence on the ratio E_ν/L in vacuum.

Normally neutrino beams are not monochromatic, so E_ν/L is not fixed. If we consider as the measurement the integrated signals (after integrating in energy the probability \times flux \times cross section), the same argument holds and a fake solution appears generically although it has a more complicated dependence on $\langle E_\nu \rangle$ and L .

Besides, the fact that other oscillation parameters will also not be known at the time of this mea-

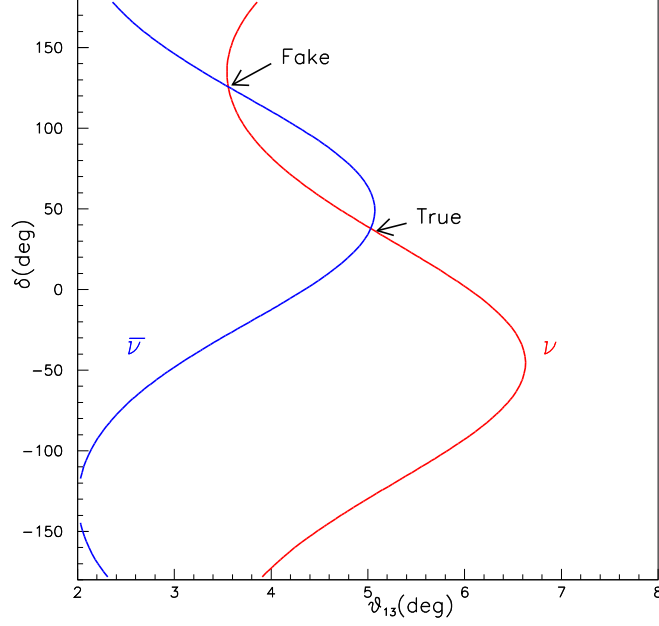


Fig. 37: Equiprobability curves $P_{\nu_e\nu_\mu}(E_\nu/L, \theta_{13}, \delta) = \text{Meas}_1$ and $P_{\bar{\nu}_e\bar{\nu}_\mu}(E_\nu/L, \theta_{13}, \delta) = \text{Meas}_2$ on the plane (θ_{13}, δ) . They generically cross at two points: the true solution (θ_{13}, δ) and a fake one.

surement, such as the $\text{sign}(\Delta m_{13}^2)$ or $\text{sign}(\cos \theta_{23})$, increases the difficulty further: these unknowns will also bias the extraction of θ_{13} and δ leading to additional fake solutions, the so-called eight-fold degeneracy [49].

Several strategies for resolving these degeneracies have been proposed. Given the energy dependence of the fake solutions, it is very useful to have a detector with good neutrino energy resolution. Figure 38 shows the oscillation probability as a function of the neutrino energy for some values of (θ_{13}, δ) with that corresponding to the fake solution $(\theta_{13}^{\text{fake}}(\langle E_\nu \rangle/L), \delta^{\text{fake}}(\langle E_\nu \rangle/L))$. The curves cross at $\langle E_\nu \rangle$ but differ quite significantly at other energies.

Another possibility is to consider performing several experiments with differing $\langle E_\nu \rangle/L$ or with different matter effects.

Finally, the measurement of other oscillation probabilities beside the golden one can help. For example, if a precise measurement of the disappearance probability for ν_e is done in the atmospheric range, with an improved Chooz-type experiment, this could provide a measurement of θ_{13} that does not depend on δ at all [50].

Similarly, if we combine the golden measurement with the silver one: $\nu_e \rightarrow \nu_\tau$ and $\bar{\nu}_e \rightarrow \bar{\nu}_\tau$, the fake solutions can be excluded [47].

5.3.2 Experimental challenge

The challenge is to measure for the first time the *small* subleading transitions $\nu_e \leftrightarrow \nu_\mu$ and $\bar{\nu}_e \leftrightarrow \bar{\nu}_\mu$ with $\langle E_\nu \rangle/L \sim |\Delta m_{\text{atmos}}^2|$. The need to be above the muon threshold implies that rather long baselines are required as shown in Fig. 39. There are many ideas being pursued. Let us briefly describe the different proposals.

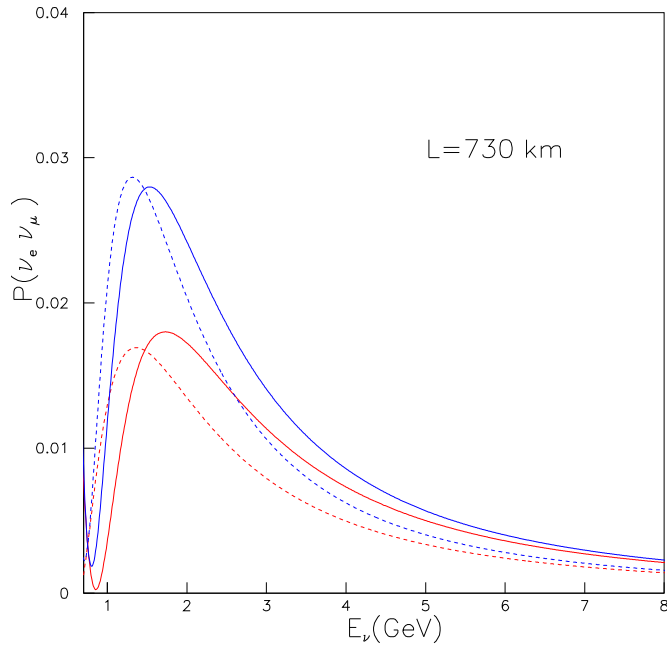


Fig. 38: Oscillation probability for neutrinos and antineutrinos as a function of the energy, for some true values of θ_{13} and δ , and for the fake solutions (dashed curves)

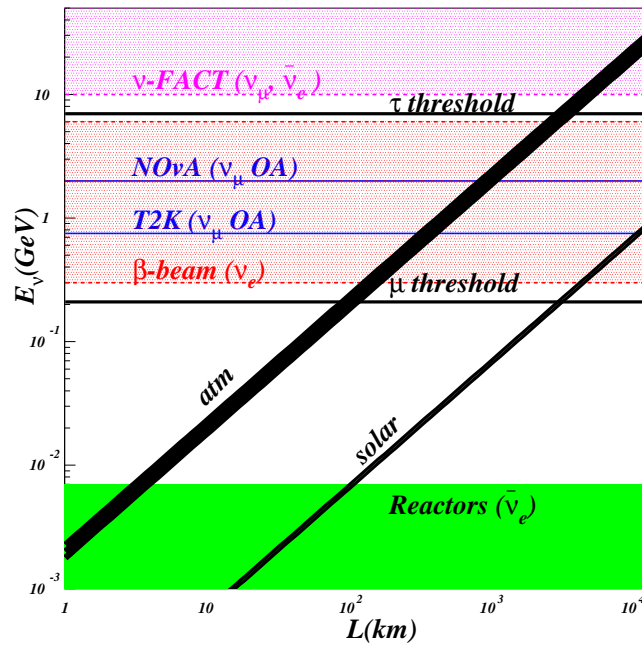


Fig. 39: Energy of the proposed future neutrino oscillation experiments: Nufact, β -beam, superbeams (T2K and NOvA) and reactors. The *atm* and *solar* black bands correspond to the first atmospheric and solar oscillation peaks, respectively.

5.3.3 Future reactor experiments

Reactor neutrinos have an energy in the range of MeV and therefore can only look at the disappearance channel $\bar{\nu}_e \rightarrow \bar{\nu}_e$. It has been pointed out before that reactor neutrinos have provided the most stringent limit on the angle θ_{13} . A future upgrade of this type of experiments is possible, by increasing the detector size and reducing the systematics by intercepting the beam with both a near and a far detector. The experiment Double-Chooz is under construction and expects to reach a sensitivity limit of $\sin^2 2\theta_{13} \geq 0.03$, with the advantage that being a disappearance measurement, there is no ambiguity due to the CP phase δ or any other parameter.

5.3.4 Future superbeam experiments

Neutrino beams produced at accelerators have already been constructed to measure the disappearance of ν_μ in the atmospheric range (K2K and MINOS), as well as the appearance channel $\nu_\mu \rightarrow \nu_\tau$ (OPERA). As we have seen, these experiments have confirmed the leading atmospheric oscillation, but they will improve the sensitivity to the unknowns very little.

These *conventional* beams result from the decay of pions and kaons produced from an intense proton beam that hits a target. They are thus mostly ν_μ (or $\bar{\nu}_\mu$ depending on the polarity) with a per cent contamination of ν_e . Neutrino beams of this type but with much higher intensity, the so-called *superbeams*, could be obtained with new megawatt proton sources, however, the sensitivity to the subleading transition $\nu_\mu \rightarrow \nu_e$ is limited by systematics. Not only can the flavour and spectral composition of these beams not be determined with good accuracy, but the irreducible background of ν_e is the limiting factor. One way to reduce this background is to use an off-axis configuration. Pion decay kinematics implies that a detector located off-axis intercepts a beam with a much better defined energy, and this allows the beam background to be reduced below the 1% level.

Two projects using off-axis superbeams are being pursued. The first one is T2K in Japan [51], that is expected to start taking data in 2009. It will use the SuperKamiokande detector to intercept a beam produced in J-PARC, which corresponds to a baseline of 295 km. If $\sin^2 2\theta_{13} \geq 0.01 - 0.02$, an appearance of ν_e will be observed, although the experiment will have no sensitivity to CP violation nor to the mass hierarchy. The second project is NOvA in the USA [52]. The NUMI beam at Fermilab will be intercepted off-axis by a new detector located 810 km away. It is expected to reach a similar sensitivity to θ_{13} as T2K, but if $\sin^2 2\theta_{13} \geq 0.05$, the comparison of the ν and $\bar{\nu}$ appearance signals could provide the first determination of the neutrino hierarchy.

5.3.5 Neutrino factory and β beams

The measurement of leptonic CP violation will probably require a further step. New ideas to obtain neutrino beams with reduced systematics have been actively discussed in recent years. At the *Neutrino Factory* (NF) [53] neutrinos are produced from μ^+ or μ^- which are accelerated to some reference energy and are allowed to decay in a storage ring with long straight sections (see Fig. 40). Subleading transitions can be searched for by looking for wrong-sign muons in a massive magnetized detector:

$$\begin{aligned} \mu^- &\rightarrow e^- \nu_\mu \bar{\nu}_e; \\ &\bar{\nu}_e \rightarrow \bar{\nu}_\mu \rightarrow \mu^+ \\ \nu_\mu &\rightarrow \nu_\mu \rightarrow \mu^-. \end{aligned} \quad (97)$$

A similar situation is found in the case of the β beam (BB) [54]. This is a neutrino beam obtained from boosted radioactive ions, such as ${}^{18}_{10}\text{Ne}$ or ${}^6\text{He}^{++}$, which are accelerated and circulated in a storage ring where they decay, producing a pure ν_e or $\bar{\nu}_e$ beam, respectively (see Fig. 41):

$${}^6\text{He}^{++} \rightarrow {}^6_3\text{Li}^{+++} e^- \quad \bar{\nu}_e$$

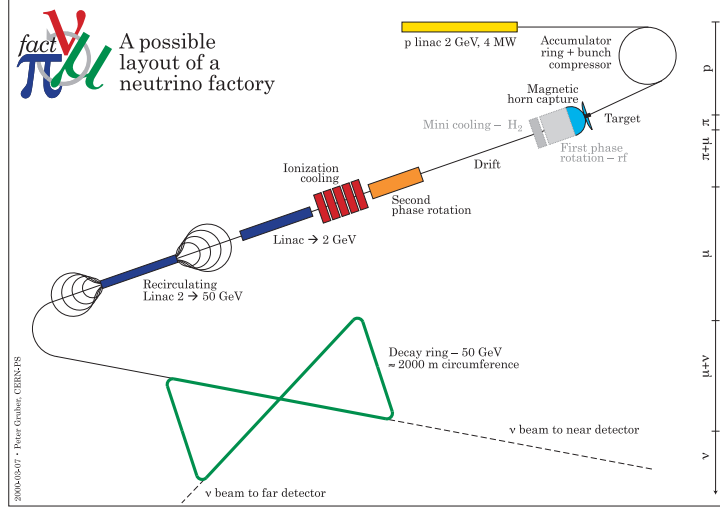


Fig. 40: Possible layout of a CERN-based Neutrino Factory complex

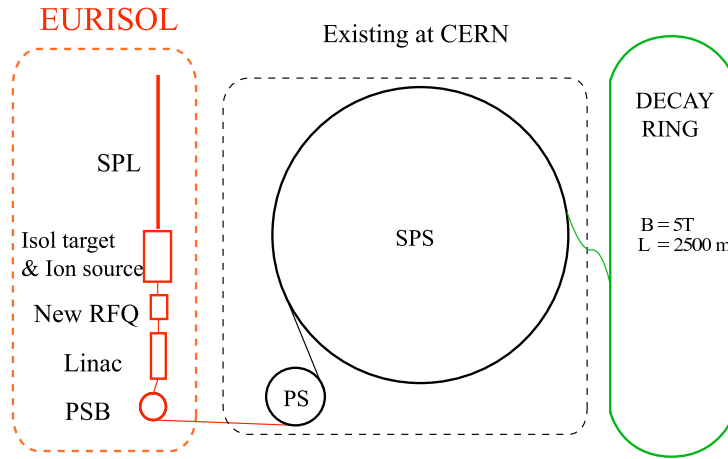
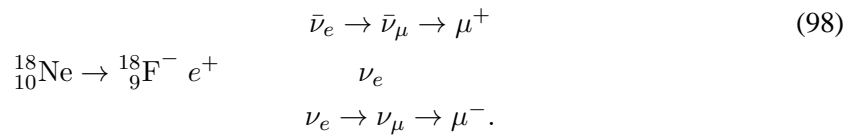


Fig. 41: Possible layout of a CERN-based β beam



The golden transition can be searched for in this case by counting muons. It is not necessary to measure their charge, so the detector does not need to be magnetized.

The neutrino fluxes ν_e and $\bar{\nu}_e$ at the NF or BB can be known with a very good accuracy, since they are easily obtained from the number of muons or ions decaying in the storage ring and the well-known muon or ion decay kinematics:

$$\left. \frac{d\Phi^{\text{NF}}}{dSdy} \right|_{\theta \simeq 0} \simeq \frac{N_\mu}{\pi L^2} 12\gamma^2 y^2 (1-y),
 \tag{99}$$

with $y = \frac{E_\nu}{E_\mu}$ and

$$\left. \frac{d\Phi^{\text{BB}}}{dSdy} \right|_{\theta \simeq 0} \simeq \frac{N_\beta}{\pi L^2} \frac{\gamma^2}{g(y_e)} y^2 (1-y) \sqrt{(1-y)^2 - y_e^2},
 \tag{100}$$

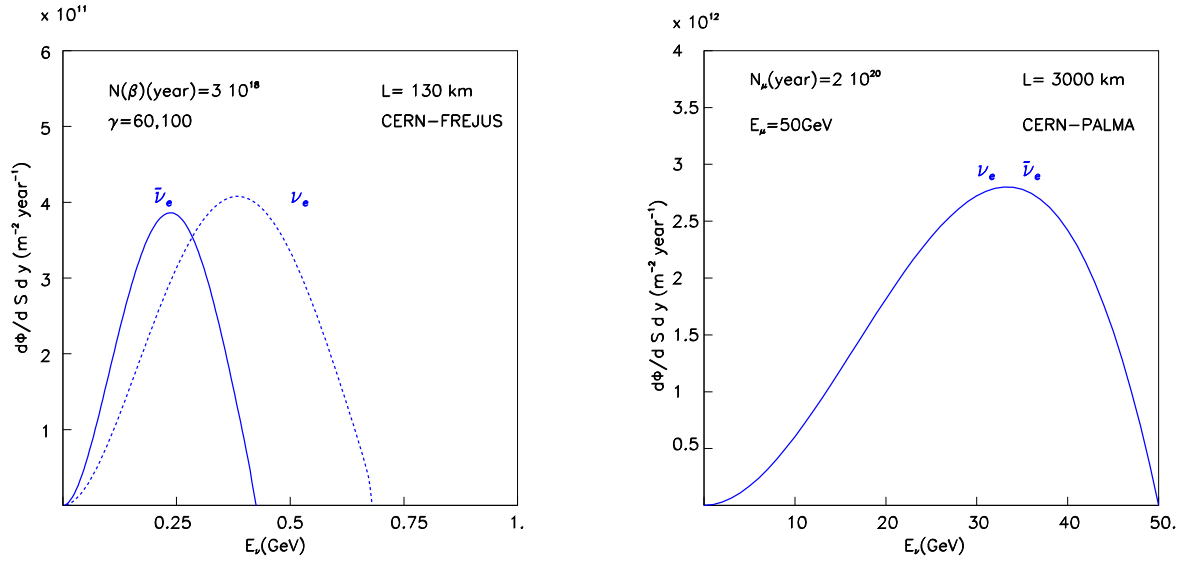


Fig. 42: Left: ν_e and $\bar{\nu}_e$ fluxes in the BB from 10^{18} $^{18}\text{Ne}/3 \times 10^{18}$ ^6He ion decays per year at $\gamma = 100/60$ and $L = 130$ km. Right: ν_e and $\bar{\nu}_e$ fluxes at the NF from 2×10^{20} $50 \text{ GeV } \mu^-/\mu^+$ decays and $L = 3000$ km.

and $y = \frac{E_\nu}{2\gamma E_0}$, $y_e = m_e/E_0$, $g(y_e) \equiv \frac{1}{60} \left\{ \sqrt{1 - y_e^2} (2 - 9y_e^2 - 8y_e^4) + 15y_e^4 \log \left[\frac{y_e}{1 - \sqrt{1 - y_e^2}} \right] \right\}$. N_μ and N_β are the muons or ions decaying per year. Note that both fluxes increase with the γ factor of the parent particle as γ^2 .

These fluxes are shown in Fig. 42 for two standard setups for the NF and the BB. Although the fluxes at the neutrino factory are larger by at least one order of magnitude, the need to magnetize the detector in the NF is a big limitation to how massive it can be in practice. In the case of the β beam no magnetization is needed, which opens the possibility to use very massive water Cherenkov detectors, like those that have been proposed to improve the limits on proton decay and to study supernova neutrinos [55].

In both the Neutrino Factory and the β -beam designs, the energy of the parent muon or ion (which is proportional to the average neutrino energy) can be optimized within a rather large range, since this is fixed by the acceleration scheme that is part of the machine design. Once the energy is fixed, the baseline is also fixed by the atmospheric oscillation length. This optimization is, however, a complex problem because there are often contradicting requirements in the maximization of the intensity, the minimization of backgrounds, having useful spectral information, measuring the *silver* channel in addition to the *golden* one, having sizeable matter effects, etc. This optimization was done for the NF some years ago and a muon energy of a few tens of GeV and a baseline of a few thousand kilometres is considered a reference setup [46]. For the BB, a scenario with a neutrino beam of a few GeV and distances of a few hundred kilometres is close to optimal.

Figure 43 shows a comparison of the physics reach for CP violation and the neutrino hierarchy of the NF and BB complexes with other second-generation superbeams that have also been proposed as alternatives (SPL, T2HK, WBB). Even though this is probably not yet the end of the story as regards optimization/comparison, these plots show that reaching the realm of $\sin^2 2\theta_{13} \sim 10^{-4}$ will be possible in the future, both for leptonic CP violation and the neutrino hierarchy.

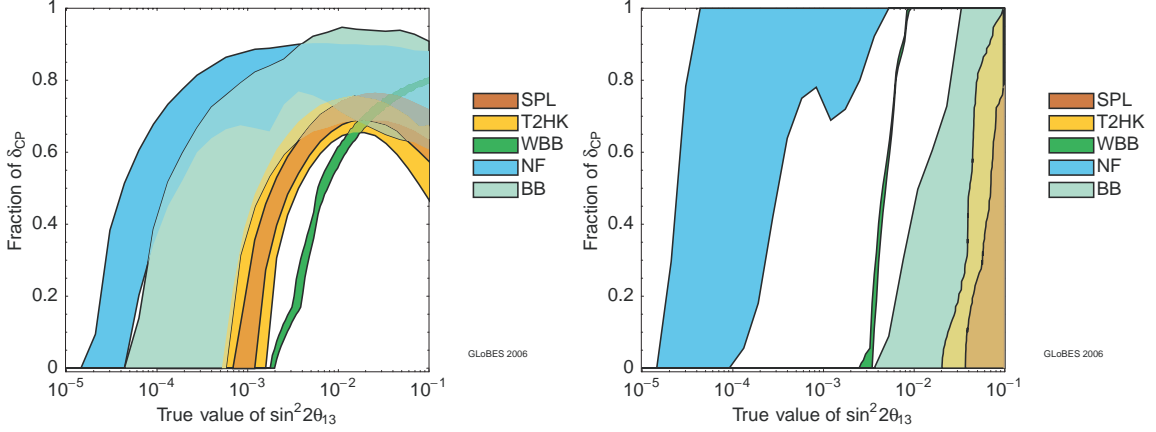


Fig. 43: Left: Sensitivity limit to leptonic CP violation in the plane $(\sin^2 2\theta_{13}, \delta)$ of superbeams (SPL, T2KHK), the wide band beam (WBB), Neutrino Factory (NF) and β beams (BB). The bands correspond to most/least conservative assumptions concerning the facility/detectors. Right: Sensitivity limits to the neutrino mass hierarchy in the same facilities. Taken from Ref. [56].

6 Leptogenesis

The Universe is made of matter. The matter–antimatter asymmetry is measured to be

$$\eta_B \equiv \frac{N_b - N_{\bar{b}}}{N_\gamma} \sim 6.15(25) \times 10^{-10}. \quad (101)$$

It has been known for a long time that all the ingredients to generate dynamically such an asymmetry from a symmetric initial state are present in the laws of particle physics. These ingredients were first put forward by Sakharov:

Baryon number violation

$B + L$ is anomalous in the SM [57] both with and without massive neutrinos, while $B - L$ is preserved if the light neutrinos are Dirac particles. At high T in the early Universe, $B + L$ violating transitions could be in thermal equilibrium [58] due to the thermal excitation of configurations with topological charge called sphalerons, see Fig. 44.

These processes violate baryon and lepton numbers by the same amount:

$$\Delta B = \Delta L. \quad (102)$$

If there are heavy Majorana singlets, as in the see-saw models, there is an additional source of L violation (and $B - L$). If a lepton charge is generated at temperatures where the sphalerons are still in thermal equilibrium, a baryon charge can be generated.

Deviation from thermal equilibrium

Sphalerons are in equilibrium for $T \geq 100$ GeV [59], which means that in order to get these processes out of equilibrium it is necessary to go to the electroweak phase transition.

Electroweak baryogenesis which has been extensively studied both in the SM and in the most popular extensions like the MSSM, is currently disfavoured in the SM because the out-of-equilibrium condition is not well met: the electroweak phase transition is not strongly first order.

A different out-of-equilibrium condition is met in the L violation processes associated to the heavy Majorana singlets [60]. These singlets are in equilibrium until they decouple at a temperature similar to their masses. Since their masses must be significantly larger than the electroweak scale if we are to explain the smallness of neutrino masses, sphalerons are still in equilibrium when the heavy Majorana

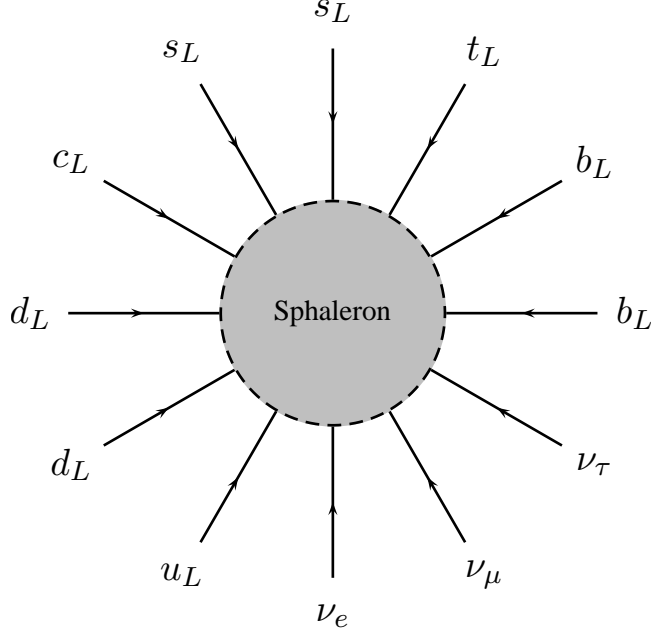


Fig. 44: Artistic view of a sphaleron

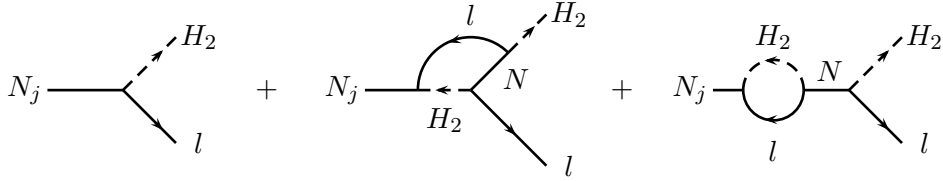


Fig. 45: Tree-level and one-loop diagrams contributing to heavy neutrino decays

singlets decouple. Therefore if a lepton number is generated in their decay, inducing a lepton number abundance Y_L , the equilibrium of sphaleron processes implies that a baryon abundance will also be present [61]:

$$Y_B = aY_{B-L} = \frac{a}{a-1}Y_L \quad a = \frac{28}{79} \quad \text{in SM.} \quad (103)$$

C and CP violation

In order for lepton number to be generated in the decay of these Majorana singlets, it is necessary that CP and C be violated in the decays:

$$\epsilon_1 = \frac{\Gamma(N \rightarrow \Phi l) - \Gamma(N \rightarrow \bar{\Phi} \bar{l})}{\Gamma(N \rightarrow \Phi l) + \Gamma(N \rightarrow \bar{\Phi} \bar{l})} \neq 0. \quad (104)$$

In fact this is generically the case since, as we have seen, there are new CP-violating phases in the neutrino mixing matrices which induce an asymmetry at the one-loop level (see Fig. 45).

These processes can then produce a net lepton asymmetry if the number distributions of the Majorana singlets, N_N , differ from the thermal ones. This can occur close to the decoupling temperature, when the density of the heavy neutrinos gets exponentially suppressed, but they are so weakly interacting that they cannot follow the fast depletion (in other words if the decay rate is slower than the expansion of the Universe close to the decoupling temperature) and

$$N_N > N_N^{\text{thermal}}. \quad (105)$$

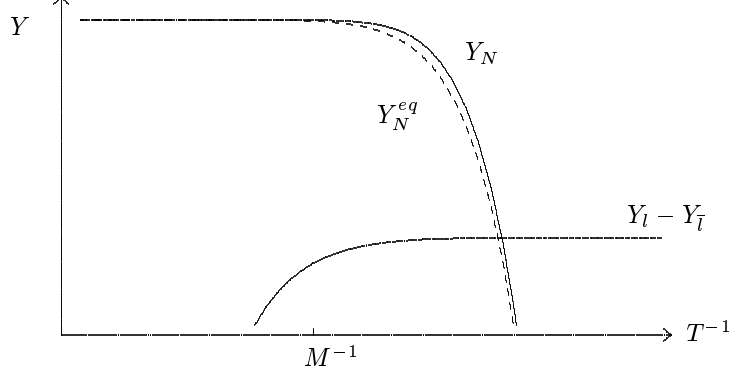


Fig. 46: Abundance of the heavy Majorana singlets at the decoupling temperature and the lepton number generated in the decay

This is shown in Fig. 46. The final asymmetry is given by

$$Y_B = 10^{-2} \underbrace{\epsilon_1}_{\text{CP-asym}} \underbrace{\kappa}_{\text{eff. factor}}, \quad (106)$$

where κ is an efficiency factor which depends on the non-equilibrium dynamics. Therefore a relation between the baryon number of the Universe and the neutrino flavour parameters in ϵ_1 exists.

An interesting question is whether the baryon asymmetry can be predicted quantitatively from the measurements at low energies of the neutrino mass matrix. Unfortunately this is not the case generically because the asymmetry ϵ_1 depends on more parameters than those that are observable at low energies.

As we saw in Section 2.1, at least three heavy Majorana neutrinos of masses M_i are needed to give masses to the three light neutrinos. The asymmetry in the decay of the lightest of them in the minimal model with $M_{2,3} \gg M_1$ is [62]

$$\epsilon_1 = -\frac{3}{16\pi} \sum_i \frac{\text{Im}[(\tilde{\lambda}_\nu^\dagger \tilde{\lambda}_\nu)_{i1}^2]}{(\tilde{\lambda}^\dagger \tilde{\lambda})_{11}} \frac{M_1}{M_i}. \quad (107)$$

Instead, at low energies, there is sensitivity only to the neutrino mass matrix:

$$\tilde{\lambda}_\nu \frac{1}{M_R} \tilde{\lambda}_\nu^T, \quad (108)$$

where M_R is the heavy Majorana mass matrix. The two combinations are different and the measurement of the matrix in Eq. (108) does not allow one to compute ϵ_1 . This is because in general the number of parameters measurable at high energies in the see-saw model is larger than at low energies. The counting of parameters for n generations before and after integrating out the heavy fields is shown Table 4 (see Section 2.3 for explanations).

If the prediction of the lepton asymmetry is not possible, it should at least be possible to constrain the neutrino mass matrix, assuming that the lepton asymmetry explains the measured baryon asymmetry.

Indeed, various upper bounds can be derived on the generated asymmetry, through a bound on ϵ_1 or on κ . In particular ϵ_1 has been shown to satisfy

$$|\epsilon_1| \leq \frac{8}{16\pi} \frac{M_1}{v^2} |\Delta m_{\text{atm}}^2|^{1/2}, \quad (109)$$

and therefore leptogenesis in this model requires that the lightest heavy neutrino is rather heavy:

$$M_1 \geq \mathcal{O}(10^9 \text{ GeV}). \quad (110)$$

Table 4: Number of physical parameters in the see-saw model with n families and the same number of right-handed Majorana neutrinos at high and low energies

	Yukawas	Field redefinitons	No. m	No. θ	No. ϕ
see-saw $E \geq M_i$	$Y_l, Y_\nu, M_R = M_R^T$ $5n^2 + n$	$U(n)^3$ $\frac{3(n^2-n)}{2}, \frac{3(n^2+n)}{2}$	$3n$	$n^2 - n$	$n^2 - n$
see-saw $E \ll M_i$	$Y_l, \alpha_\nu^T = \alpha_\nu$ $3n^2 + n$	$U(n)^2$ $n^2 - n, n^2 + n$	$2n$	$\frac{n^2-n}{2}$	$\frac{n^2-n}{2}$

A sufficiently large κ implies an upper bound on the lightest neutrino mass:

$$m_i \leq \mathcal{O}(\text{eV}). \quad (111)$$

For further details and references see Ref. [62].

7 Outlook for theory

One of the most important questions to resolve in neutrino physics is whether the origin of neutrino masses is a new physics scale and if so what this scale is. One can envisage various possibilities for such new physics, and the simplest is to assume that its associated energy scale is above the electroweak scale. It is well known, since the pioneering work of Weinberg [63], that the appropriate language to describe the low-energy effects of such new physics, no matter what it is, is that of *effective field theory*. The effects of *any* beyond-the-standard-model dynamics with a characteristic energy scale, $\Lambda \gg v$, can be described at low-energies, i.e., $E < \Lambda$, by the SM Lagrangian plus a tower of operators with mass dimension, $d > 4$, constructed out of the SM fields and satisfying all the gauge symmetries. Even though the number of such operators is infinite, they can be classified according to their dimension, d , since an operator of dimension d must be suppressed by the scale Λ^{d-4} , and therefore higher dimensionality means stronger suppression in the high-energy scale:

$$\mathcal{L} = \mathcal{L}_{\text{SM}} + \sum_i \frac{\alpha_i}{\Lambda} \mathcal{O}_i^{d=5} + \sum_i \frac{\beta_i}{\Lambda^2} \mathcal{O}_i^{d=6} + \dots \quad (112)$$

Different fundamental theories correspond to different values for the *low-energy couplings* α_i, β_i, \dots , but the structure of the effective interactions is the same.

It turns out that the first operator in the list is the famous Weinberg operator of Eq. (10):

$$\mathcal{O}^{d=5} = \bar{L}_L^c \tilde{\Phi}^T \tilde{\Phi} L_L, \quad (113)$$

where $\tilde{\Phi}, L$ are the SM Higgs and lepton doublets, respectively. This operator is the only one with $d = 5$ in the SM, and, as we have seen, brings in three essential new features to the minimal SM:

- neutrino masses,
- lepton mixing,
- lepton number violation.

Upon spontaneous symmetry breaking, such an operator induces a neutrino mass matrix of the form

$$m_\nu = \alpha \frac{v^2}{\Lambda}, \quad (114)$$

where α is generically a matrix in flavour space. Neutrino masses are therefore expected to be naturally small if $\Lambda \gg v$.

If we assume that the neutrino masses we have measured are the result of this leading operator, one could ask the question: What type of new physics would induce such an interaction? In the same way that one can conjecture the presence of a massive gauge boson from the Fermi four-fermion interaction, one can classify the extra degrees of freedom that can induce at tree-level Weinberg's interaction. It turns out that there are the three well-known possibilities as depicted in Fig. 47:

- type I see-saw: SM+ heavy singlet fermions [6],
- type II see-saw: SM + heavy triplet scalar [64],
- type III see-saw: SM + heavy triple fermions [65],

or combinations. The masses of the extra states define the scale Λ .

It is also possible that Weinberg's interaction is generated by new physics at higher orders, such as in the famous Zee model [66] and related ones [67]. In this case, the coupling α in Eq. (112) will be suppressed by loop factors $1/(16\pi^2)$.

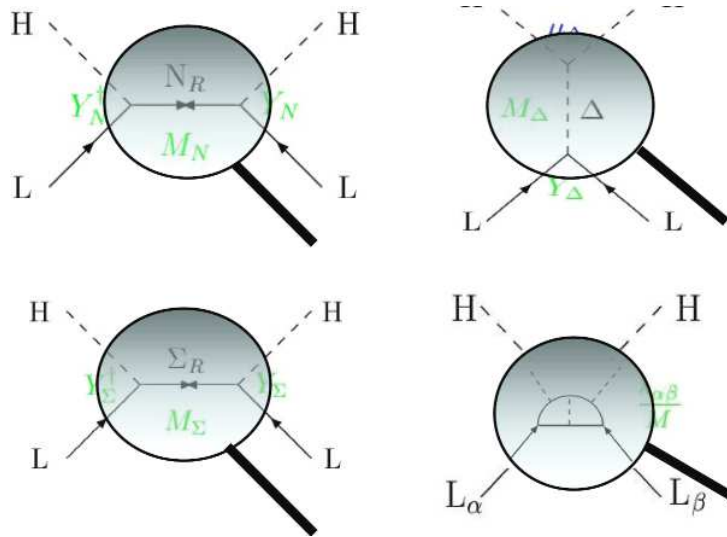


Fig. 47: Magnifying-glass view of Weinberg operator in see-saws Type I (top left), Type II (top right), Type III (bottom left) and Zee-Babu model (bottom right)

Unfortunately the measurement of neutrino masses alone will not tell us which of these possibilities is the one chosen by Nature. In particular, the measurement of Weinberg's interaction leaves behind an unresolved $\alpha \leftrightarrow \Lambda$ degeneracy that makes it impossible to know what the scale of the new physics is, even if we were to know the absolute value of neutrino masses.

Generically, however, the new physics will give other signals beyond Weinberg's operator. The next in importance are the $d = 6$ operators of Eq. (112) [68]. Recently the $d = 6$ operators induced at tree level in see-saw models of Types I to III have been worked out [69]. They give rise to a rich phenomenology that could discriminate between the models. In particular, they could induce beyond-the-standard-model signals in Z and W decays, deviations in the ρ parameter or the W mass, and mediate

rare lepton decays, as well as violations of universality and unitarity of the neutrino mass matrix. It would therefore be extremely important to search for these effects. Whether they are large enough to be observed or not depends strongly on how high the scale Λ is, since all these effects are suppressed by two powers of Λ .

As mentioned before, neutrino masses alone do not tell us what Λ is, but there are several theoretical prejudices of what this scale should be. The most popular one is to relate Λ to a grand-unification scale, given the intriguing fact that the seesaw-type ratio $\frac{v^2}{M_{\text{GUT}}} \sim 0.01 - 0.1$ eV, in the right ballpark of a neutrino mass scale. Recently, however, it has been pointed out [70] that within see-saw models, and without supersymmetry, this choice would destabilize the electroweak scale, since the Higgs mass would receive quadratic loop corrections in Λ . A naturalness argument would then imply that $\Lambda < 10^7$ GeV, at least if there is no supersymmetry.

Another possibility is to consider Λ to be related to the electroweak scale, i.e., not far from it. After all, the electroweak scale is the only scale we are sure exists. The question is then if such a choice would be testable via the measurement of the $d = 6$ operators. The answer to this question is no in the simplest type I see-saw model, because in order to get neutrino masses in the right ballpark when $\Lambda \sim \text{TeV}$, it is necessary to have extremely small Yukawa couplings, which suppress also the $d = 6$ operators to an unobservable level. Several recent works have discussed the possibility to have larger effects of the $d = 6$ operators [69, 71, 72]. One possibility is that realized in Zee-type models where $d = 5$ operators are forbidden at tree level and are therefore suppressed by loop factors, while $d = 6$ operators are allowed at tree level and therefore unsuppressed. A more radical possibility is the existence of two independent scales in Eq. (112), one that suppresses $d = 6$ operators, Λ_6 , and another one, $\Lambda_5 \gg \Lambda_6$, that suppresses the $d = 5$ one. This possibility is not unnatural, because the $d = 5$ and $d = 6$ operators can be classified according to a global symmetry: total lepton number. If we therefore assume that the scale at which lepton number is broken, Λ_{LN} , is much higher than the scale at which lepton flavour violation, Λ_{LFV} , is relevant, we can ensure that the $d = 5$ operator, that breaks lepton number, is suppressed by the former scale, $\Lambda_5 \sim \Lambda_{\text{LN}}$, while the lepton-flavour effects induced by operators of $d = 6$ would be suppressed only by a lower scale $\Lambda_6 \sim \Lambda_{\text{LFV}} \ll \Lambda_{\text{LN}}$. The effective field theory describing such a possibility would look therefore like

$$\mathcal{L} = \mathcal{L}_{\text{SM}} + \sum_i \frac{\alpha_i}{\Lambda_{\text{LN}}} \mathcal{O}_i^{d=5} + \sum_i \frac{\beta_i}{\Lambda_{\text{LFV}}^2} \mathcal{O}_i^{d=6} + \dots, \quad (115)$$

where the operators that break lepton number and those that preserve this symmetry are generically suppressed by different scales. Such a possibility has recently been considered in the context of the popular Minimal Flavour Violation hypothesis [72]. The underlying rationale for such an assumption is not completely ad hoc, since in this context one could hope to explain two apparently contradictory facts

- common origin of lepton and quark family mixing at a scale Λ_{LFV} ,
- large gap between neutrino masses and remaining fermions since neutrino masses would be suppressed by Λ_{LN} .

In fact this separation of scales is built-in in several of the models mentioned before. The simplest example being the type II see-saw model, where the scalar-triplet mass, M_Δ , is directly connected with the Λ_{LFV} , while the scale of lepton number violation is M_Δ^2/μ , where μ is a dimensionful coupling in the scalar potential of the triplet. In fact, it is the separation of scales that makes the phenomenology of this model much richer at low energies than that of type I see-saw models in their simplest version.

If this possibility is realized, there would be many interesting consequences:

- lepton flavour violation could be measurable beyond neutrino oscillations,
- the scale of lepton flavour violation, Λ_{LFV} , could be reached at the LHC.

In recent years a lot of activity has been devoted to studying possible signals of neutrino masses at the LHC. Lepton number violation could give rise to spectacular signals at LHC, like same-charge lepton pairs [73]. This signal has been studied in detail recently in various see-saw models. In one-scale models of type I, neutrino masses restrict these processes to being highly suppressed beyond detectable levels [74]. However, the separation of scales mentioned before, allows light enough triplets in the type II see-saw to be pair-produced at LHC:

$$pp \rightarrow H^{++}H^{--} \rightarrow l^+l^+l^-l^-, \quad (116)$$

leading to the powerful signal of same-charge lepton pairs. Not only can the invariant mass be reconstructed from the two leptons pairs, but the flavour structure of the branching ratios to different leptons is in one-to-one correspondence with the flavour structure of the neutrino mass matrix. Therefore the putative measurement of these processes would provide direct information on the neutrino mass matrix [75].

Solving the flavour problem of the Standard Model is surely a quixotic enterprise and we shall need to explore as many avenues as we can. In recent years it has become increasingly clear that in addition to quark flavour factories, we can obtain very valuable information on different aspects of this puzzle also from LHC and lepton flavour factories.

8 Conclusions

The results of many beautiful experiments in the last decade have demonstrated beyond doubt that neutrinos are massive and mix. The standard 3ν scenario can explain in terms of four fundamental parameters all available data, except that of the unconfirmed signal of LSND. The lepton flavour sector of the Standard Model is expected to be at least as complex as the quark one, even though we know it only partially.

The structure of the neutrino spectrum and mixing is quite different from the one that has been observed for the quarks: there are large leptonic mixing angles and the neutrino masses are much smaller than those of the remaining leptons. These peculiar features of the lepton sector strongly suggest that leptons and quarks constitute two complementary approaches to understanding the origin of flavour in the Standard Model. In fact, the smallness of neutrino masses can be naturally understood if there is new physics beyond the electroweak scale.

Many fundamental questions remain to be answered in future neutrino experiments, and these can have very important implications for our understanding of the Standard Model and of what lies beyond: Are neutrinos Majorana particles? Are neutrino masses the result of a new physics scale? Is CP violated in the lepton sector? Could neutrinos be the seed of the matter–antimatter asymmetry in the Universe?

A rich experimental programme lies ahead where fundamental physics discoveries are very likely (almost warrantied). We can only hope that neutrinos will keep up with their old tradition and provide a window to what lies beyond the Standard Model.

References

- [1] Lectures, *Field Theory and the Standard Model*, V. Rubakov at this School.
- [2] C. Amsler *et al.*, Phys. Lett. B667 (2008) 1. <http://pdg.lbl.gov>.
- [3] Ch. Weinheimer *et al.*, Phys. Lett. B460 (1999) 219; Erratum *ibid.* 464 (1999) 332; M. Lobashev *et al.*, Phys. Lett. B464 (1999) 227.
- [4] K.A. Assamagan *et al.*, Phys. Rev. D53 (1996) 6065.
- [5] R. Barate *et al.*, Eur. Phys. J. C2 (1998) 395.
- [6] P. Minkowski, Phys. Lett. B 67 (1977) 421; M. Gell-Mann, P. Ramond and R. Slansky, in *Supergravity*, edited by P. van Nieuwenhuizen and D. Freedman, (North-Holland, Amsterdam, 1979), p. 315; T. Yanagida, in *Proceedings of the Workshop on Unified Theories and Baryon Number in*

- the Universe*, edited by O. Sawada and A. Sugamoto (KEK Report No. 79-18, Tsukuba, 1979), p. 95; R.N. Mohapatra and G. Senjanović, Phys. Rev. Lett. 44 (1980) 912.
- [7] B. Pontecorvo, Zh. Eksp. Teor. Fiz. 33 (1957) 549; JETP, 6 (1958) 429; Zh. Eksp. Teor. Fiz. 33 (1958) 247.
- [8] Z. Maki, M. Nakagawa and S. Sakata, Prog. Theor. Phys. 28 (1962) 870.
- [9] L. Baudis *et al.*, Phys. Rev. Lett. 83(1999) 41.
- [10] H.V. Klapdor-Kleingrothaus and I.V. Krivosheina, Mod. Phys. Lett. A21 (2006) 1547.
- [11] C. Arnaboldi *et al.*, Phys. Rev. Lett. 95 (2005) 142501.
- [12] R. Arnold *et al.*, Nucl. Phys. A781 (2007) 209.
- [13] L. Wolfenstein, Phys. Rev. D17 (1978) 2369.
- [14] S.P. Mikheev and A.Yu. Smirnov, Yad. Fiz. 42 (1985) 1441; Nuov. Cim. 9C (1986) 17.
- [15] J. Bahcall, P.I. Krastev and A. Yu. Smirnov, JHEP 0105 (2001) 015. J.N. Bahcall, M.C. González-García and C. Peña-Garay, JHEP 0108 (2001) 014.
- [16] J.N. Bahcall, M.H. Pinsonneault and S. Basu, Astrophys. J. 555 (2001) 990.
- [17] B.T. Cleveland *et al.*, Astrophys. J. 496 (1998) 505.
- [18] W. Hampel *et al.*, Phys. Lett. B447 (1999) 127.
- [19] J.N. Abdurashitov *et al.*, J. Exp. Theor. Phys. 95 (2002) 181.
- [20] Y. Fukuda *et al.*, Phys. Rev. Lett. 77 (1996) 1683.
- [21] S. Fukuda *et al.*, Phys. Rev. Lett. 86 (2001) 5651 and 5656; Phys. Lett. B539 (2002) 179; M.B. Smy *et al.*, Phys. Rev. D69 (2004) 011104.
- [22] Q.R. Ahmad *et al.*, Phys. Rev. Lett. 87 (2001) 071301; 89 (2002) 011301 and 011302; 92 (2004) 181301.
- [23] B. Aharmim *et al.*, Phys. Rev. C72 (2005) 055502. B. Aharmim *et al.*, Phys. Rev. Lett. 101 (2008) 111301.
- [24] K. Eguchi *et al.*, Phys. Rev. Lett. 90 (2003) 021802.
- [25] S. Abe *et al.*, Phys. Rev. Lett. 100 (2008) 221803.
- [26] C. Arpesella *et al.*, Phys. Rev. Lett. 101 (2008) 091302.
- [27] M. Honda, *et al.*, Phys. Rev. D 54 (1995) 4985. V. Agrawal, T.K. Gaisser, P. Lipari, and T. Stanev, Phys. Rev. D 53 (1996) 1314. M. Honda *et al.*, Phys. Rev. D 70 (2004) 043008.
- [28] Y. Fukuda *et al.*, Phys. Lett. B335 (1994) 237.
- [29] R. Becker-Szendy *et al.*, Nucl. Phys. (Proc. Suppl.) B38 (1995) 331.
- [30] M. Sánchez *et al.*, Phys. Rev. D 68 (2003) 113004.
- [31] M. Ambrosio *et al.*, Phys. Lett. B566 (2003) 35.
- [32] Y. Fukuda *et al.*, Phys. Rev. Lett. 81 (1998) 1562.
- [33] M. Ishitsuka for the Super-Kamiokande Collaboration, Proceedings of the XXXIXth Rencontres de Moriond on Electroweak Interactions and Unified Theories (2004), hep-ex/0406076.
- [34] Y. Ashie *et al.*, Phys. Rev. Lett. 93 (2004) 101801.
- [35] M.H. Ahn, Phys. Rev. Lett. 90 (2003) 041801.
- [36] B. Achkar *et al.*, Nucl. Phys. B434 (1995) 503.
- [37] F. Boehm *et al.*, Phys. Rev. D64 (2001) 112001.
- [38] M. Apollonio *et al.*, Phys. Lett. B 466 (1999) 415; Eur. Phys. J. C27 (2003) 331.
- [39] A. Aguilar *et al.*, Phys. Rev. D 64 (2001) 112007.
- [40] B. Armbruster *et al.*, Phys. Rev. D65 (2002) 112001.
- [41] A. A. Aguilar-Arevalo *et al.* [MiniBooNE Collaboration], Phys. Rev. Lett. 100 (2008) 032301.
- [42] M.C. González-García and M. Maltoni, Phys. Rep. 460 (2008) 1.

- [43] G. L. Fogli *et al.*, Phys. Rev. D 78 (2008) 033010 .
- [44] A. Osipowicz *et al.*, hep-ex/0109033.
- [45] For a recent review see P. Vogel, arXiv:0807.2457[hep-ph].
- [46] A. Cervera *et al.*, Nucl Phys. B579 (2000) 17.
- [47] A. Donini, D. Meloni and P. Migliozzi, Nucl. Phys. B646 (2002) 321.
- [48] J. Burguet-Castell *et al.*, Nucl Phys. B608 (2001) 301.
- [49] H. Minakata and H. Nunokawa, JHEP 0110 (2001) 1. G.L. Fogli and E. Lisi, Phys. Rev. D54 (1996) 3667. V. Barger, D. Marfatia and K. Whisnant, Phys. Rev. D65 (2002) 073023.
- [50] H. Minakata *et al.*, Phys. Rev. D68 (2003) 033017.
- [51] Y. Itow *et al.*, Nucl. Phys. Proc. Suppl. 111 (2002) 146.
- [52] A. Para and M. Szeleper, hep-ex/0110032; D. Ayres *et al.*, hep-ex/0210005.
- [53] S. Geer, Phys. Rev. D57 (1998) 6989. A. De Rújula, M.B. Gavela, and P. Hernández, Nucl. Phys. B547 (1999) 21.
- [54] P. Zucchelli, Phys. Lett. B532 (2002) 166.
- [55] M. Goodman, *et al.*, Physics Potential and feasibility of UNO, ed. D. Casper, C.K. Jung, C. McGrew and C. Yanagisawa, SBHEP01-3 (July 2001).
- [56] The ISS Physics Working Group, “Physics at a future Neutrino Factory and super-beam facility,” Editors S.F. King, K. Long, Y. Nagashima, B.L. Roberts, and O. Yasuda, arXiv:0710.4947 [hep-ph].
- [57] G. 't Hooft, Phys. Rev. Lett. 37 (1976) 8.
- [58] V.A. Kumin, V.A. Rubakov, and M.E. Shaposhnikov, Phys. Lett. B155 (1985) 36.
- [59] D. Bödecker, M. Laine, and K. Rummukainen, Phys. Rev. D 61 (2000) 056003.
- [60] M. Fukugita, and T. Yanagida, Phys. Lett. B 174 (1986) 45.
- [61] J.A. Harvey and M.S. Turner, Phys. Rev. D 42 (1990) 3344.
- [62] For a recent review and further references see S. Davidson, E. Nardi, and Y. Nir, Phys. Rep. 466 (2008) 105 [arXiv:0802.2962 [hep-ph]].
- [63] S. Weinberg, Phys. Rev. Lett. 43 (1979) 1566.
- [64] M. Magg and C. Wetterich, Phys. Lett. B94 (1980) 61; J. Schechter and J. W. F. Valle, Phys. Rev. D 22 (1980) 2227; C. Wetterich, Nucl. Phys. B187 (1981) 343; G. Lazarides, Q. Shafi, and C. Wetterich, Nucl Phys. B181 (1981) 287; R.N. Mohapatra and G. Senjanović, Phys. Rev. D23 (1981) 165.
- [65] R. Foot, H. Lew, X.-G. He, and G.C. Joshi, Z. Phys. C44 (1989) 441; E. Ma, Phys. Rev. Lett. 81 (1998) 1171.
- [66] A. Zee, Phys. Lett. B93 (1980) 389.
- [67] A. Zee, Phys. Lett. B161 (1985) 141 and Nucl.Phys. B264 (1986) 99. K.S. Babu, Phys. Lett. B203 (1988) 132.
- [68] W. Buchmuller and D. Wyler, Nucl. Phys. B 268 (1986) 621.
- [69] A. Abada, C. Biggio, F. Bonnet, M. B. Gavela, and T. Hambye, JHEP 0712 (2007) 061.
- [70] F. Vissani, Phys. Rev. D57 (1998) 7027; J. A. Casas, J. R. Espinosa, and I. Hidalgo, JHEP 0411 (2004) 057.
- [71] J. Kersten and A. Y. Smirnov, Phys. Rev. D 76 (2007) 073005.
- [72] V. Cirigliano, B. Grinstein, G. Isidori, and M.B. Wise, Nucl. Phys. B 728 (2005) 121.
- [73] W. Y. Keung and G. Senjanovic, Phys. Rev. Lett. 50 (1983) 1427.
- [74] F. del Aguila, J. A. Aguilar-Saavedra, and R. Pittau, JHEP 0710 (2007) 047.
- [75] T. Han and B. Zhang, Phys. Rev. Lett. 97 (2006) 171804. T. Han, B. Mukhopadhyaya, Z. Si, and K. Wang, Phys. Rev. D 76 (2007) 075013. J. Garayoa and T. Schwetz, JHEP 0803 (2008) 009.

M. Kadastik, M. Raidal, and L. Rebane, Phys. Rev. D 77 (2008) 115023. A. G. Akeroyd, M. Aoki, and H. Sugiyama, Phys. Rev. D 77 (2008) 075010. P. Fileviez Perez, T. Han, G. y. Huang, T. Li, and K. Wang, Phys. Rev. D 78 (2008) 015018.